The Drosophila ovarian terminal filament imports lipophilic molecules that regulate follicle development within its ovariole

Bhawana Maurya and Allan C Spradling

[1]Howard Hughes Medical Institute Research Laboratory

Carnegie Institution for Science

3520 San Martin Dr., Baltimore, MD 21218

ABSTRACT

Oogenesis in Drosophila is regulated by hormones and neuropeptides acting directly and indirectly on the ovary. But how regulatory molecules reach individual developing follicles within sheath-encased ovarioles is less well understood. The terminal filament (TF) forms a specialized somatic structure positioned at the anterior end of ovarioles in virtually all insect ovaries, but physiological roles TFs play in adult ovaries remain unclear. By knocking down, specifically in the TF, the organic anion transporters Oatp74D and Oatp30B, we found that the TF is a major provider of both ecdysone and other lipophilic molecules needed for germ cell differentiation and follicle development. The exocyst component Sec6 is also essential for TF function and when disrupted, vesicles back up at the TF-germ cell junction, suggesting that endosomes move between the stacked TF and cap cells by transcytosis. We propose that TFs and ovariolar sheaths allow follicles in each ovariole to develop optimally in locally coordinated environments that still respond to changes in systemic and external conditions.

Keywords: ecdysone, stem cell niche, germline stem cell, Oatp30B, ovariole

INTRODUCTION

Ovaries in Drosophila, like most insect species, comprise a semi-autonomous collection of ovarioles, each containing germline cysts and ovarian follicles lined up assembly line fashion, in developmental order (reviewed in Büning, 1994). Characteristically, each ovariole starts with a "terminal filament (TF)," described in the earliest study of an insect ovary by Malphigi in 1669 (see Gall, 1996) but whose functional significance in egg production has remained unclear (Figure 1A). TF cells are flattened like a stack of coins, and their number varies between species (Büning, 1994; Sarikaya et al. 2011). The well studied Drosophila TF contains 8-9 somatic cells that protrude from the end of each ovariole anteriorly, while posterior cells contact cap cells (Figure 1A).

Terminal filaments form in early third instar (L3) larval ovaries when precursor cells intercalate in the nascent ovariole (Godt and Laski, 1995; Sahut-Barnola et al. 1995). TF precursors express two similar and essential BTB domain transcription factors *bric-a-brac 1* and *2 (bab1 and bab2)* starting prior to stack formation (Godt and Laski, 1995), and soon also express the signaling molecule *hedgehog (hh)* (Forbes et al. 1996). As stacks reach their final size, TF cells complete germline stem cell (GSC) niche production by specifying cap cells (CCs) at the TF base (Figure 1A; Forbes et al. 1996; Zhu and Xie, 2003; Song et al. 2007; review Hsu et al. 2019). Apical ovarian cells then migrate down to define ovarioles, enclosing germ cells, and surrounding them with sheaths (Cohen et al. 2002). Subsequently, beginning at the pupal stage, the division rate of GSCs and differentiation of their daughters into germline cysts determines oocyte production by an ovariole throughout adult life.

The steroid hormone ecdysone controls multiple events in egg production beginning with the GSC niche, GSC division and the onset of cyst production (Ables and Drummond-Barbosa,

2010) much as it regulates larval and pupal development (Kannangara et al. 2021; Scanlan et al. 2023). In mature follicles, upregulation of *shd*, which encodes an E-20-monooxygenase in follicle cells, generates active 20OH-ecdysone (Petryk et al. 2003), an essential prerequisite for ovulation (Knapp et al. 2020). Like in vertebrates, Drosophila follicles persist in the ovary after ovulation and transform into a steroid-producing corpus luteum (Deady and Spradling, 2015; Knapp et al. 2020). Ovarian follicle development is also modulated by insulin (Drummond-Barbosa and Spradling, 2001), prostaglandins (Tomalla et al. 2025), and juvenile hormone (Luo et al. 2021; Kurogi et al. 2023). Neuropeptides produced in the brain, fat body and gut maintain harmony with the external environment (Hartenstein et al. 2006; Hughson et al. 2021; Zhu et al. 2024; Li et al. 2024).

Cells require the organic anion transporter Oatp74D/SLCO1A2 to take up and respond to ecdysone (Okamoto et al. 2018). During adult oogenesis, at least three periods of 20-hydroxy-ecdysone reception activity have been identified in follicles at specific stages (Buszczak et al. 1999; Carney and Bender, 2000; Terashima et al. 2005; Sun et al. 2008; Ables and Drummond-Barbosa, 2010; König et al. 2011; Morris and Spradling, 2012; Domanitskaya et al. 2014; Deady et al. 2015; Drummond Barbosa, 2019; Hsu et al. 2019; Ghosh et al. 2025). The ecdysone that activates the later steps of oogenesis is produced stage-specifically in ovarian follicle cells. Except for local synthesis, how ecdysone, prostaglandins, neuropeptides and other regulatory molecules reach early developing germ cells and follicles remains incompletely understood, despite the importance of signal delivery (Hatori et al. 2021). There is no evidence of ecdysone movement between adjacent follicles or of intake from nearby ovarioles or the hemolymph.

A germline organelle, the fusome, is essential for germline cyst formation in both sexes in Drosophila, and marks future oocytes in Drosophila, vertebrates and many other organisms

(King et al. 1968; Büning, 1994; Davidian and Spradling, 2025; Pathak and Spradling, 2026). The Drosophila fusome contains multiple isoforms of the the *hu-li tai shao (hts)* gene (Petrella et al, 2007) and additional proteins, including the recycling endosome protein rab11 (Lighthouse and Spradling, 2008). Fusome proteins are already present in migrating primordial germ cells before they reach the gonad and dramatically increase further beginning as GSCs in a rab11-dependent manner, but sources beyond de novo synthesis have not been proven. Cysts maintain contact with a series of stationary escort cells (Morris and Spradling, 2011) until they reach the start of region 2b halfway through the germarium. Here cysts shed EC membranes and pass two follicle stem cells (FSCs) that each donate a single daughter cell that proliferate to cover the follicle (Figure 1A, green).

Rapid germline growth, cyst production, and yolk formation require abundant phospholipids, steroids and other lipids (DiMario and Mahowald, 1987; Sieber and Spradling, 2015; Sieber et al. 2016; McMillan et al. 2018). In many systems, reserves for these purposes are sequestered in lipid droplets (LDs) (review: Welte, 2015). These dynamic organelles also buffer metabolic stress and protect cells from oxidative damage (Olzmann and Carvalho, 2019; Walther and Farese, 2012; Welte and Gould, 2017). Intestinal enterocytes and adipocytes release lipoprotein particles that circulate in the insect hemolymph bound to lipophorin (Obniski et al. 2018; Carrera et al. 2025). These lipoproteins are taken up by cells via lipophorin receptors (LpRs), including LpR2, which functions analogously to mammalian LDL receptors to mediate lipoprotein endocytosis (Palm et al., 2012; Sieber and Spradling,, 2015; Matsuo et al. 2019). Once internalized, lipids are distributed and recycled through endosomal and secretory pathways. Vesicle-mediated transport is central to lipid trafficking, and the exocyst complex is a key regulator of polarized secretion and membrane delivery (Heider and Munson, 2012; Wu and

Guo, 2015). In addition, organic anion transporting polypeptides (OATPs) import additional lipophilic molecules into cells besides ecdysone, including other steroid-related hormones, prostaglandins and ecosinoids (Hagenbuch and Stieger. 2013; Granados et al. 2021). In mammals, the Slco5a1 transporter is of prognostic significance in serous ovarian cancer (Svoboda et al. 2018), and is orthologous to Drosophila Oatp30B.

By knocking down genes specifically in the TF, we show that TF-mediated import of ecdysone and other lipophilic molecules is essential to maintaining germ cell development and their lipid droplet reserves within ovarioles. Our findings argue that by supplying hormones and lipid precursors, terminal filaments organize and modulate stem cells, cysts and follicles enclosed with their individual ovariole sheaths, to maintain oocyte quality and maximize female gamete production.

METHODS

Fly Genetics

All *Drosophila melanogaster* stocks were maintained on standard cornmeal agar media at room temperature unless otherwise specified. The Oregon R strain was used as the wild-type control throughout the study. Enhancer trap lines (PZnnnnn) are from Karpen and Spradling (1992); R11A12 is described in (Jenett et al, 2012; www.janelia.org/gal4-gen1). The GAL4 driver lines *bab1-GAL4*, *c587-GAL4*, and *nanos-GAL4* were obtained from the Bloomington Drosophila Stock Center (BDSC). UAS-RNAi lines were obtained from the Vienna Drosophila Resource Center (VDRC), including *Sec6-RNAi* (VDRC #22077), *Sec15-RNAi* (VDRC #35161), *Sec10-RNAi* (VDRC #318483), *Sec5-RNAi* (VDRC #28873), *Exo70-RNAi* (VDRC #103717), *Exo84-RNAi* (VDRC #108650), *Oatp74D*-RNAi (V#37295), *Oatp30B-RNAi* (VDRC #110237), LpR2 (VDRC #25684) and *ACC-RNAi* (VDRC #8105), ATPα (VDRC#12330). All genetic

crosses were performed at 25 °C unless otherwise noted. For temporally controlled gene knockdown, the temperature-sensitive Gal80 system (*tub-GAL80^{ts}*) was used in combination with *bab1-GAL4*. Crosses were maintained at 18 °C to allow GAL80^{ts} mediated repression of GAL4 activity during development. Adult progeny was then shifted to 29 °C to inactivate GAL80^{ts} and permit GAL4 driven RNAi expression at desired developmental stages.

Egg Laying Assay

Newly eclosed (0–1 day old) flies were maintained in plastic bottles containing molasses plates overlaid with a layer of wet yeast, replaced daily. For egg laying measurements, five pairs of flies were kept per bottle, and the number of eggs laid was counted every 24 hours, in triplicate.

Immunostaining:

Immunostaining was performed on ovaries dissected from adult *Drosophila melanogaster* females. Dissections were carried out in Grace's insect medium, followed by fixation in 4% paraformaldehyde (PFA) with 0.01% PBST (PBS with 0.01% Triton X-100) for 30 minutes at room temperature. Fixed ovaries were then blocked in 5% Normal Goat Serum (NGS) for 1 hour and incubated overnight at 4°C with primary antibodies diluted in blocking solution. After extensive washing with PBST, samples were incubated with secondary antibodies (1:200 dilution) for 2 hours at room temperature. DNA was counterstained with DAPI (0.5 µg/mL), and samples were mounted in Vectashield mounting medium. Confocal images were acquired using a Leica STELLARIS 8 DIVE microscope. Intensity profile graphs were generated using Image J (NIH) and GraphPad Prism software.

The following primary antibodies were used: mouse anti-Hts (1:100; DSHB), chicken anti-α5 (1:200; DSHB), mouse anti-LaminC (1:50; DSHB), rabbit anti-Cytochrome C (1:50; Cell

Signaling Technology), chicken anti-GFP (1:200; aveslabs) and rabbit anti-Hedgehog (1:500; kindly provided by Dr. Tom Kornberg).

Nile Red, BODIPY 493/503 and LipidTOX™ Deep Red Staining

To visualize neutral lipids, tissues were dissected in 1× PBS and fixed in 4% paraformaldehyde for 20 minutes at room temperature. Samples were washed three times with 1× PBS and incubated in Nile Red solution (1 µg/mL in PBS), LipidTOX™ Deep Red (1:500), BODIPY 493/503 (1 µg/mL in PBS) for 30 to 45 minutes in the dark. After staining, tissues were washed briefly with PBS, counterstained with DAPI (0.5 µg/mL), and mounted in Vectashield for imaging. Images were acquired using a confocal microscope.

FM1-43 staining

Ovaries were dissected in ice-cold 1× PBS and incubated in FM1-43FX dye (5 µg/mL in PBS; Thermo Fisher) for 15–20 minutes at room temperature in the dark. After staining, tissues were washed briefly with PBS and fixed in 4% paraformaldehyde for 20 minutes. Following fixation, samples were washed three times with PBS and mounted in Vectashield for imaging.

DHE and MitoSox Staining

To assess reactive oxygen species (ROS) levels, freshly dissected ovaries were incubated in Schneider's Drosophila medium containing either dihydroethidium (DHE; 5µM, Invitrogen) or MitoSOX™ Red (5 µM, Invitrogen) for 10–15 minutes at room temperature in the dark. After staining, tissues were washed twice with 1× PBS and fixed in 4% paraformaldehyde for 20 minutes. Samples were then rinsed, mounted in Vectashield with DAPI, and imaged using a confocal microscope.

Quantification of lipid droplet number and volume in the germarium

Lipid droplets in the germarium were quantified using ImageJ. Confocal Z-stacks of BODIPY 493/503, Nile Red and LipidTOX™ stained ovaries were acquired with identical imaging settings across all genotypes. Maximum intensity projections were generated and converted to 8-bit images. The germarium was manually outlined and analysis was restricted to this region. Images were thresholded using the adjust threshold function with identical threshold parameters applied to all samples within an experiment, and converted to binary masks. Lipid droplets were quantified using the analyze particles function with a size threshold of 0.07 μm^2 to infinity (corresponding to droplets ≥0.3 µm in diameter). Total LD number per germarium was recorded and data were exported for statistical analysis. Individual lipid droplet volumes were measured using the volume calculator plugin in ImageJ, which estimates volume from the droplet area and optical section thickness, and total lipid content per germarium was calculated by summing all droplet volumes.

Confocal imaging, image acquisition and processing

A Zeiss LSM 780 laser-scanning confocal microscope (Carl Zeiss) with a 20x and 43x oil-immersion objective (Carl Zeiss) was used for data collection. Confocal z stacks were obtained in 1 mm intervals at a resolution of 1024×1024. Images were processed with Zen software (Zeiss) to obtain maximum projections. Fiji were used for image rotation and cropping.

Statistical Analysis:

Graphs and statistical analyses were performed using GraphPad Prism (GraphPad Software). For comparisons between two groups, a two-tailed unpaired Student's *t*-test was used. For comparisons among three or more groups, one-way analysis of variance (ANOVA) was

performed. A p-value < 0.05 was considered statistically significant. The sample size (n), statistical test used, and exact p-values are indicated in the corresponding figure legends. A minimum of n = 3 independent biological replicates was analyzed for each statistical comparison. Data are presented as mean ± s.e.m. unless otherwise stated.

RESULTS

The terminal filament expresses hormone importers and neuroendocrine receptors

We surveyed libraries of reporter gene expression (Karpen and Spradling, 1992; Janett et al. 2012, and ovarian single-cell RNA seq studies that included the TF (Sladina et al. 2020; Sladina et al. 2021) to identify candidate genes potentially relevant to lipophilic gene import. Oatp74D, which is required for ecdysone uptake (Okamoto et al. 2018), is expressed highly in pupal ovary TFs and at lower levels in adults. Oatp30B (Figure 1B), in contrast, increases more than 10-fold from pupal levels, to become the most highly expressed Oatp family member in the adult TF. Many Oatp family members interact with the sodium potassium ATPase in transporting substrates (Sweet et al. 2007; Reinhard et al. 2021) and ATPalpha also showed TF localization (Figure 1C).

In addition, several neuropeptide receptors that have been implicated in Drosophila ovarian regulation were found to be specifically expressed in the TF. Dh44-R2, the Drosophila ortholog of mammalian corticotrophin releasing hormone (CRF) receptor 1, which regulates vertebrate oogenesis (Gershon et al. 2025), is specifically expressed in the TF (Figure 1D). The Allatostatin C/somatostatin receptor 2 (Kubrak et al. 2022) is required for ovarian circadian behavior (Zhang et al, 2021). An AstC-R2 reporter is expressed in the TF (Figure 1F). The cenB1A gene, expressed in Dh44 neurons of the pars intercebralis, is also TF expressed and regulates lipid levels (Nath et al. 2025) (Figure 1E).

Ovarian germ cells in the germarium and previtellogenic follicles contain lipid droplets:

Large lipid droplets, as described in previous reports for more mature follicles, were visualized in early ovarian cells within the germarium following staining with BODIPY 493, Nile red or LipidTox which stain primarily neutral lipids (Figure1G-I). LDs accumulate prominently within within GSCs, CBs, cysts and ovarian follicles positioned downstream from the TF and CCs (Figure1G-I). Quantitative analysis revealed that germ cells contained the most LDs, and these droplets preferentially stained with BODIPY (Figure 1J). An EM that fortuitously captured a cross-section of a posterior TF cell cytoplasm and a cap cell shows the presence of numerous small vesicles, potentially indicative of vesicular trafficking in TF cells (Figure K, arrow).

Oatp74D is required in the TF for normal follicle development

We tested Oatp74D function within TF cells by driving Oatp74D RNAi using *bab1-GAL4,GAL80*^{ts}, a driver strongly specific for TF and cap cells in the ovary (Figure 2A). Flies were raised at 18°C to ensure GAL4 repression by GAL80, but the temperature was raised to 29°C between day 1 and day 3 of adult development to knock down Oatp74D expression during this interval. Normally, a germarium contains only 2 GSCs and about 1 CB with round spectrosomes (Figure 2B, marked with arrow). However, germaria from Oatp74D^{KD} ovaries contained many germ cells whose fusome staining indicated that GSCs continued to divide, but cyst development was arrested in early stages (Figure 2C-D, G, marked with arrow and arrowhead). These experiments argue that the terminal filament imports ecdysone into the ovariole that is needed for normal germ cells development.

Because pupae normally express higher levels of Oatp74D than adults, we also knocked down Oatp74D expression between 48h APF and analyzed on adult day 3 (Figure 2E vs F). The

longer period of transporter knockdown resulted in strong defects extending to follicles which failed to bud properly (Figure 2F, arrow). A reduced number of tumorous cysts suggested that GSC divisions were also reduced. Fewer LDs was present following both periods of Oatp74D knockdown (Figure 2H).

Oatp30B is essential for cyst differentiation, LD acquisition and Hh signaling

Next we explored the role of the other major organic anion importer family member present in the TF, Oatp30B. Following 2 days of Oatp30B knockdown we observed at least 12 cells with a single, or two connected spectrosomes (2-cell cysts), indicating that Oatp30B^{KD} spared GSC division, but arrested cyst development in region 2a (Figure 2I, arrows). This effect was highly significant (Figure 2J). None of the remaining cells contained LDs, showing that Oatp30B activity is required, at least indirectly, to maintain LDs. LDs were lost between 24 and 48 hours after temperature shift (Figure 2K-R), a rate of loss of about 2.4 μm^3/24 hours (Figure 2S-T). Thus, Oatp30B imports molecules into the TF whose loss have an even greater effect on germ cell development and LD maintenance than knockdown of the ecdysone importer Oatp74D.

Hedgehog (Hh) signaling by TF cells is important for ovariole development in larval ovaries and in adults it stimulates FSC maintenance and division (Forbes et al. 1996a). Consequently, we examined whether some of the effects of Oatp30B^{KD} were mediated by changes in Hh. We found that Hedgehog (Hh) levels are lower in Oatp30B^{KD} ovaries (Figure 3B, B') compared to controls (Figure 3A, A') and the reduction of about two fold was significant (Figure 3C). Hh is modified by cholesterol and palmitate, and its proper secretion and gradient formation depend on lipid availability (Porter et al. 1996). Therefore, Oatp30B mediated uptake of lipophilic cargos, might be needed to maintain normal levels of Hh processing, secretion, and

signaling in TF cells. However, Hh alterations cannot explain the drastic inhibition of germ cell differentiation, suggesting that a different molecule imported by Oatp30B is needed for cyst formation.

Some Oatp family members specifically interact with the Na-K-ATPase in transporting cargos (Torrie et al. 2004; Reinhard et al. 2011). We tested to see if knocking down ATPα showed the same defects as Oatp30B (Figure 3E-F). As with Oatp30B KD, the number of arrested cysts showing spectrosomes was increased (Figure 3D), and the number of LDs was reduced, but the magnitude of the changes was lower. We could not conclude if ATPα worked directly with Oatp30B, but they affected the same developmental events. Loss of membrane potential can activate Hh signaling (Emmons-Bell and Hariharan, 2021), but Hh overexpression produces a very different effect than the Oatp30^{KD} phenotype (Forbes et al. 1996a).

LpR2 is needed to maintain LD levels and germ cell development in the germarium

We also examined the role in the TF of LpR2, a low-density lipoprotein (LDL) receptor (Matsuo et al., 2019) which functions in ovarian cells during lipid yolk formation (Parra-Peralbo and Culi, 2011; Sieber and Spradling, 2015). When LpR2 was knocked down in the TF as before LD levels were reduced to low levels by day 3 (Figure 3G). A complete time course showed that LD number was reduced to a basal level by 30 h (Figure S1). We also measured total germ cell lipid droplet (LD) volume over time to estimate the rate of LD-mediated lipid transfer from terminal filament to the germarium (Figure 3H). LD lipid volume declined by about 1.6 μm^3 between 6 and 12 hours post-knockdown, followed by a further reduction of ~1.4 μm^3 during the subsequent 6 hour interval.

Knockdown of LpR2 in terminal filament cells also caused distinctive defects in cyst development. By 12 hours post-knockdown an inhibition and even reversion of cyst development was indicated by the appearance of GSC like single germ cells in region 2a (Figure S1A-C). By 24h cysts were reduced in number and their fusomes were less branched compared to controls (arrows, Figure S1A-H). By 30h, LDs were mostly gone and cyst development was sparse and abnormal throughout the germarium (Figure S1J). Thus, TF-specific depletion of LpR2 disrupts LD homeostasis and completely blocks further cyst production and development.

We noticed that TFs in pupal and very young adult ovaries contained another type of small vesicle that stained strongly with the fusome protein Hts (Figure 3I). These vesicles were completely absent after 2 days of adult development and did not recur (Figure 3J-K). They raise the possibility that the TF transports more diverse cargos than currently described, including vesicles that contribute to fusome production or growth. Both Hts protein and its partner alpha-Spectrin are unlikely to be supplied in this manner in adults, however. Hts protein is absent in ovarian germ cells in hts mutants (Lin et al. 1994) and alpha-Spectrin is absent in adult germline clones of an alpha-spectrin mutant (deCuevas et al. 1996).

Terminal filament and cap cells transport lipid-rich vesicles in germ cells via exocyst-dependent vesicle trafficking:

Terminal filament cells uptake lipophilic molecules from the hemolymph through Oatp30B and LpR2, but the mechanism by which these lipids are delivered to the germarium remains unclear. The stacked organization of the TF suggests that TF cells would need to transfer lipids taken up from the hemolymph into cap cells by undergoing a series of exocytosis and endocytosis events that resulted in the directional movement of cargos.

When exosomes are released into extracellular space through exocytosis, the exocyst complex represents a key effector of polarized movement, as it is responsible for tethering secretory vesicles to specific plasma membrane domains prior to fusion (Meek et al. 2024). Although the exocyst is used by most or all cells, and is critical for cytokinesis in mitotically cycling cells, adult TF and CC cells do not cycle or divide and appear fully differentiated from late pupal stage of ovary development. Sec6 is a key exocyst component due to its binding to Sec9 at the plasma membrane and to Rtnl1 in the ER, is crucial for exocyst assembly (Morgera et al. 2012, Dubuke et al.2015).

We initially looked for a Sec6 requirement, by knocking down Sec6 using *bab1-Gal4* and observed a severe depletion of mature oocytes in the ovary and daily egg production never exceeded low levels (Figure S2A). Additionally, we used FM1-43 dye which labels vesicles undergoing membrane recycling and regulated exocytosis (Ramachandran and Budnik, 2010) to confirm that TF and CC has active exocytosis (Figure S2B). FM1-43 is widely used in studies of synaptic activity and neurogenesis, where it marks vesicle turnover during neurotransmitter release. *Sec6* knockdown significantly reduced FM1-43 signal in TF cells (Figure S2C vs S2B, D).

To gain further insight into endocytic transport in TF and CC cells we used *bab1-GAL4, tub-Gal80^{ts}* for temporal control, in late pupae when these cells are fully differentiated. Females maintained at 18 °C were shifted to 29 °C in late pupae and analyzed in 3d adults. LD levels were strongly reduced throughout the germarium, as revealed by BODIPY 493/503 staining (Figure 4B,E) compared to control (Figure 4A,E). Interestingly, while LDs were depleted from germ cells, large LDs accumulated specifically in posterior TF and cap cells in *Sec6* knockdown animals where they are rarely observed in controls (Figure 2B’ vs 2A’). Quantitative analysis

confirmed that LD size and number increased significantly in the TF region (Figure 2F; Figure S2E-F, G). Knockdown of 5 other exocyst components (*Sec10*, *Sec15*, *Sec5*, *Exo70*, *Exo84*) also resulted in LD depletion (Figure S3 A-F, G), but only Sec6 depletion consistently caused LD backup near the CC/GSC border. Sec6 knockdown also abrogated normal cyst and follicle development (Figure 4C-D). Together these finding show that exocyst-mediated lipid delivery from TF and CC is essential for germ cell and cyst development.

Escort cells contribute little to supporting LDs in the germarium.

To determine whether TF and CC are the primary sources of lipid supplied to germ cells, or whether escort cells also contribute, we used the *hh-GAL4* driver, which is expressed in TF, CC, and escort cells (Figure 4G-G'). Knockdown of *Sec6* using *hh-GAL4* resulted in a pronounced depletion of lipids from the germarium. In particular, lipid accumulated specifically in TF and CC cells, but not escort cells (Figure 4H-I, J) further supporting the TF and cap cells as a lipid entry pathway based on endocytic activity.

We also tested the *c587-GAL4* driver to inactivate Sec6 in escort cells, FSCs and early follicle cells, but not TF and cap cells (Figure 4K, K'). No buildup of LDs in the escort cells were observed, and the levels of LDs in the germarium were similar to controls (Figure 4L-M, N).

Temporal dynamics of material transfer from TF and CC cells during cyst production

We analyzed the kinetics of neutral lipid transfer from TF and CC cells into germarial lipid droplets, by measuring the effects of *Sec6* knockdown every 6-hours following temperature shift. Flies were shifted from 18 °C to 29 °C at day1 and analyzed to determine both LD number and volume (Figure 5B-K, 5A control). These experiments revealed several new insights (Figure 5L-O). First, LDs rapidly backup in the TF and CC reaching a plateau in just 12 hours which is

maintained thereafter (Figure 5N). At the same time LD movement out of the TF and CC cells ceases at 12h, we began to observed LD numbers decrease in the germarium (Figure 5 L). Thus, LDs levels in the germarium first dropped between 12h and 18h and further decreases were observed every subsequent 6 hr period (Figure 5L) until LD number stabilized after 20h. Bodipy stained lipid in the TF plateaued at 12 hours (Figure 5O), and level of total lipid in the germarium began to fall shortly thereafter (Figure 5M).

However, after the TF ceased lipid transport, lipid levels dropped in a region-specific manner (Figure 5P) rather than showing a anterior to posterior polarity. This regional specificity probably reflected region-specific rates of metabolic activity that in the absence of sufficient production resulted in LD depletion (Fig. 5B-F, P). The slowest losses were in region 2a, where cells are slowing progressing in leptotene-zygotene and have previously been shown to have relatively low metabolism and gene expression. In contrast, in region 3, cells are completing nurse cell transfer, follicle formation and embarking on rapid follicle growth. By ~36 h, when LD depletion was nearly complete, defects in 16-cell cyst formation became evident in region 2b (Fig. 5Q). These findings show that LDs can act as a buffer for a significant time period, but also that there is no checkpoint or signaling system that can respond to prevent the onset of developmental abnormalities. Effects of sec6 mediated depletion were also observed for the transient Hts-positive vesicles present only during days 1-2 (Figure S4).

Lipid droplets in the germarium protect against mitochondrial ROS accumulation

We hypothesized that the continuous lipid supply from the terminal filament is required not only to meet energetic demands of early germ cells, but serve functions beyond energy storage. We have observed that LDs in early germ cells are frequently in close proximity to mitochondria in the germarium (Figure 6A, encircled in yellow). This spatial association is consistent with

earlier reports suggesting that LD-mitochondria contacts facilitate fatty acid transfer**,** enabling mitochondrial respiration and regulating oxidative homeostasis (Rambold et al., 2015; Bailey et al. 2015; Nguyen et al., 2017; Avila et al. 2025).. Disruption of these contacts or LD content has been linked to elevated mitochondrial reactive oxygen species (ROS) and organelle dysfunction.

To directly test whether loss of lipid droplets leads to ROS accumulation**,** we knocked down the lipogenic gene Acetyl-CoA Carboxylase (ACC) in germ cells using *nanos-GAL4.* ACC is a key enzyme in de novo fatty acid synthesis and is essential for neutral lipid production. ACC knockdown resulted in a dramatic reduction or complete loss of LDs throughout the germarium (Figure 6C vs B; D). We next assessed mitochondrial ROS using MitoSOX and DHE staining. Both assays showed significantly elevated ROS levels in *ACC*-depleted germarium compared to controls (Figure 6E,F,K,L,H,I), indicating oxidative stress resulting from lipid depletion.

To determine whether this ROS phenotype also arises when LD transport from the TF is impaired, we examined TF-specific knockdown of *Sec6*. As previously shown, *Sec6* knockdown blocks vesicular transport of lipids to the germarium. Consistent with our hypothesis, *Sec6*-RNAi in TFs also led to elevated mitochondrial ROS in germ cells, as measured by both MitoSOX and DHE (Figure 6E,G,H,I,K,L), which ultimately affects cyst development and follicle formation.

DISCUSSION

The terminal filament imports lipophilic molecules using transporters to support GSC activity

Our experiments demonstrate that a major function of the Drosophila terminal filament and cap cells is to import and deliver ecdysone and other molecules from the outside into the anterior ovariole (Figure 7A). Molecules entering via the TF are delivered immediately to the the GSC, downstream germ cells, and anterior escort cells. Ecdysone is known to directly regulates GSC

division and maintenance independently of other factors such as insulin (Ables and Drummond-Barbosa, 2010). Ecdysone reception is also needed in escort cells for germline cyst formation and meiotic entry (Konig et al. 2011; Morris and Spradling, 2012).

We found that knocking down the ecdysone transporter Oatp74D did not immediately stop GSC division, but did prevent the completion of normal cyst formation. Previously, it was not clear how ecdysone was provided for its early ovarian functions, and our results indicate that import via the TF is essential. Interestingly, disruption of Oatp30B, which has the capacity to import sterols and other lipophilic molecules such as prostaglandins, almost immediately stopped cyst formation while GSC divisions continued, generating a GSC tumor. This suggested that at least one molecule dependent on Oatp30B activity is more critical for initiating GSC differentiation and cyst formation than the ecdysone imported by Oatp74D. This function may explain why these importers reverse their relative abundance in TF cells between pupae and adults (Sladina et al. 2020; Sladina et al. 2021).

The terminal filament also supports early follicle development within its ovariole

Rapid GSC division and cyst formation that takes place under rich nutritional conditions requires a substantial input of lipids to support the new membrane production required. Our experiments showed that the TF plays a major role in simply providing raw materials for cell proliferation. Without the activity of LpR2 in the TF, large LDs normally found in germline and somatic cells were not maintained. LpR2 is a major importer of triglycerides (TGs) which make up a large fraction of LD lipids. Depletion of Oatp30B also prevented LD maintenance. The rapid disappearance of LDs following LpR2 KD or Oatp30B KD in the TF was probably caused by their ongoing utilization by growing somatic and germ cells. The speed with which LDs decrease, quantitated here (Figure 2S,T; Figure 3H; Figure S1J), indicates that the TF must

provide a substantial ongoing supply of triglycerides and possibly other lipophilic molecules to maintain the steady state LD level observed under normal circumstances.

GSCs and later germ cells highly express Fabp (Pang et al. 2023), encoding fatty acid binding protein, the major Drosophila fatty acid transporter, suggesting that germ cells receive TGs from the TF and deliver them farther down the ovariole. Many of the imported molecules, such as LD constituents, likely originate in the gut, may have been transiently stored in the fat body, and were transferred to the TF via the hemolymph. However, other tissues such the extensive sheath surrounding the terminal filament and germarium (Figure 1K), may also store and modify some potentially unique TF-bound molecules prior to uptake.

How far along the ovariole might the influence of TF importation extend? Due to its proximity and absence of a known alternative supply, the TF can now be considered the leading candidate to provide the ecdysone needed for inducing apoptosis of excess germline cysts near the region 2a/2b border in the germarium under declining nutrition conditions (Drummond-Barbosa and Spradling, 2001). We observed that Oatp74D depletion affected the entire germarium, follicle budding, and the development of early follicles. Ecdysone biosynthesis by ovarian somatic also plays a role, and its magnitude and regulation are poorly known. A similar checkpoint requiring ecdysone and insulin acts at stage 8. It may represent the last step influenced by ecdysone from the TF. Border cell migration during stage 9 depends on the ecdysone biosynthesis gene Phantom. Substantial production of ecdysone clearly takes place in follicle cells of stage 10 follicles (Buszczak et al. 2000; Sun et al. 2008; Sieber and Spradling, 2015). This generates enough ecdysone that some can be taken up and stored in association with yolk proteins for maternal release, and plays multiple roles in egg completion (reviewed in Berg et al., 2024).

Oogenesis is almost certainly independent of the TF during these late stages. Ecdysone production from stage 10 follicles ensures there will be large amounts of sterols and trigycerides available to form lipid yolk. In newly eclosed flies ecdysone from developing follicles is thought to induce a female metabolic state, by entering the hemolymph, moving to the brain and and increasing female feeding behavior (Sieber and Spradling, 1995). Females begin to consume far more nutrients than males and load their hemolymph with lipoprotein particles, which are stored in the fat body and taken up by oocytes via the yolkless receptor (DiMario and Mahowald, 1987). Even just 24hr of feeding on a rich food source generates enough stored reserves to support egg production long after the food source has been fully consumed. In newly eclosed flies with few stage 10 follicles, larval fat body cells that fill the abdomen of young flies may provide the ecdysone needed to stimulate initial feeding and lipid production.

Terminal filament conservation likely serves the universal need to rejuvenate oocytes

Until recently, the importance and conservation of early oogenesis stages taking place prior to the onset of meiosis have not been widely appreciated. Primordial germ cells or GSC daughters start oogenesis by constructing and polarizing germline cysts as prerequisites for specifying oocytes and nurse cells in both higher insects, amphibians, and mammals (reviewed in Spradling et al. 2025). Terminal filament conservation may reflect its critical contributions to these processes, by bringing in lipids needed to rebuild cell membranes, and steroids required as conserved regulators.

These studies highlighted multiple ways that LDs assist from the very beginning in building the oocyte. LDs transport lipids that support the rapid production of new germ cell plasma and organelle membranes, including ER-rich germ cell fusomes. Initially, less new membrane may be required in somatic cells, because stable escort cells can likely use their thin

membranes to support multiple passing cysts. Additionally, LDs may function as depots to maintain redox balance in early germ cells. LDs have the potential to buffer excess free fatty acids, distribute lipids to mitochondria in a regulated manner, and prevent lipotoxic stress. In the absence of LDs, free fatty acids can undergo peroxidation**,** triggering a cascade of oxidative damage (Listenberger et al., 2003; Bailey et al., 2015). LDs are known protect against oidative damage in the nervous system by transporting peroxidated lipids to glial cells for removal (Moulton et al. 2021).

We found that germ cell LDs likely play a similar role in the germarium. Both ACC knockdown in germ cells and TF-specific Sec6 knockdown increased mitochondrial ROS, demonstrating that disruption of LD accumulation compromises redox homeostasis. This aligns with prior observations that LD–mitochondria contacts facilitate fatty acid transfer and protect against ROS accumulation (Nguyen et al., 2017; Rambold et al., 2015). Thus, lipid provisioning may enable biosynthetic and energetic demands while safeguarding germ cells from oxidative damage.

<u>The ovary may be regulated by brain neuropeptides via the TF</u>

We also documented the expression of several genes in the terminal filament, including Dh44-R2, AstC-R2, and cenB1A (Figure 1C-E) that suggest the TF receives information from the brain and other tissues via G-protein coupled receptors that allow it to modulate temporal aspects of follicle production. Dh44-R2 is orthologous to mammalian corticotrophin releasing factor receptor (Crfr1) which along with their conserved ligands Dh44/CRF (diuretic hormone 44/corticotrophin releasing factor) and urocortins 1 and 2 are major regulators of the mammalian reproductive and urinary system (review Mavridis et al. 2025). In Drosophila these highly

conserved signaling systems have been studied in the brain and urinary system (Zandawalla et al. Cannell et al. 2016) but not in the ovary.

Dh44 is expressed in Malphigian tubule principal cells and regulates urinary output in conjunction with the Na-K-ATPase and the water channel Drip (Johnson et al. 2005; Cannell et al. 2016; Lee et al. 2023). These cells express six different Oatp family members including Oatp53Db which was implicating in expelling the toxic cardioglycoside ouabain from principal cells, protecting Drosophila from its toxic effects on the Na-K-ATPase (Torrie et al. 2004). Since this study showed TF-enriched expression of ATPα, Dh44-R2, cenB1A (which is expressed along with Dh44-R2 in Dh44 neurons), and also the Drip water channel are TF enriched (Sladina et al. 20; Sladina 24). These results indicate that Dh44 may regulate the gonad as well as the Malphigian in Drosophila, like CRF in mammals, and indicates that further studies are warranted.

Terminal filaments allow a level of ovariolar independence

Subdivisions with gonads that favor development in sequential strings are common among many species. In mammalian testes, seminiferous tubules show highly organized development along the tubule, and certain stage pairs lie close to each other in a consistent manner as the tubule winds is way back and forth through the testis (Yoshida, 2020). Follicle development in sequential order may be advantageous because it allows a complex series of steps dependent on the amount and quality of available food and water to be optimized in light of multiple constraints. Follicle spacing determines the number of simultaneously developing follicles and hence metabolic demand, ovarian dimensions that must fit in the abdominal cavity, and a female's weight which must remain low enough for flight despite a full load of eggs. Flight is essential to the fly's ecological strategy, since rich but rare, dispersed and changing food sources

and ovulation sites must be found. The terminal filaments allow ovarioles to operate semi-autonomously, almost as independent small ovaries (Figure 7B). This makes it relatively easy to maximize the movement and spacing within each ovariole to help address constraints, while sharing the final functions of ovulation and fertilization using just two oviducts and a single uterus. Above all, a blockade or injury to the operation of any one ovariole has a negligible effect on overall fecundity.

CONCLUSION

We show that the terminal filament is an entry port for hormones including ecdysone, for lipid droplet constituents, and likely for many other molecules. The TF is directly connected to the germline stem cell niche which the hormones regulate and the precursors supply. The high conservation of the TF across insects matches the high conservation of early oogenesis, including germline cyst formation, meiotic entry and follicle formation which enable oocytes to undergo "rejuvenation" and produce a new generation as highly fit as its predecessor. In particular, the TF provides the ecdysone via the importer Oatp74D that is needed to even begin oocyte development by making a germline cyst. Disrupting the activity of other TF importers and interacting molecules, like the Na-K ATPase, identified other parts of this regulatory and supply system. Finally, the separate regulation of the generative region of each ovariole gives semi-autonomy to each developing egg string, providing new insight into the sophistication with which follicle development in ovaries is managed, steps that are likely to be necessary during gametogenesis in a wide phylogenetic span of animals.

ACKNOWLEDGEMENTS

We thank Mahmud Siddiqi for assistance with light microscopy and Mike Sepanski for electron microscopy. Dianne Williams assisted with Drosophila stock management. We are grateful to Asya Davidian, Haolong Zhu, Madulika Pathak, Ashish Tiwari, Yunpeng Fu, Andy Mao and other members of the Spradling laboratory for discussions. Allan Spradling is an Investigator of the Howard Hughes Medical Institute, and HHMI provided support for these studies. The Carnegie Institution for Science has generously supported the Spradling lab in Baltimore for many years, for which we are grateful.

REFERENCES

Ables ET, Drummond-Barbosa D. (2010). The steroid hormone ecdysone functions with intrinsic chromatin remodeling factors to control female germline stem cells in Drosophila. Cell Stem Cell 7, 581–592. doi: 10.1016/j.stem.2010.10.001.

Avila, A., Lewandowski, A.S., Li, Y., Gui, J., Lee, K.A., Yang, Z., Kim, M., Lyles, J.T., Man, K., Sehgal, A., Chandler, J.D., Zhang, S.L. (2025). A carnitine transporter at the blood-brain barrier modulates sleep via glial lipid metabolism in Drosophila. Proc. Natl. Acad. Sci. U.S.A. 122(4): e2421178122.

Bailey AP, Koster G, Guillermier C, Hirst EMA, MacRae JI, Lechene CP, Postle AD, AP Gould. (2015). Antioxidant role for lipid droplets in a stem cell niche of Drosophila. Cell, 163, 340–353.

Berg C, Sieber M, Sun J. (2024). Finishing the egg. Genetics 226: iyad183. doi: 10.1093/genetics/iyad183.

Buszczak M, Freeman MR, Carlson JR, Bender M, Cooley L, Segraves WA. (1999). Ecdysone response genes govern egg chamber development during mid-oogenesis in Drosophila. Development 126, 4581-9. doi: 10.1242/dev.126.20.4581.

Büning J. (1994). The Insect Ovary: Ultrastructure, Previtellogenic Growth and Evolution.Chapman and Hall. DOI:https://doi.org/10.1007/978-94-011-0741-9.

Carney GE, Bender M (2000) The Drosophila ecdysone receptor (EcR) gene is required maternally for normal oogenesis. Genetics 154(3):1203–1211.

Carrera P, Odenthal J, Risse KS, Jung Y, Kuerschner L, Bülow MH. (2025). The CD36 scavenger receptor Bez regulates lipid redistribution from fat body to ovaries in Drosophila. Development 151, dev202551. doi: 10.1242/dev.202551.

Cohen ED, Mariol MC, Wallace RM, Weyers J, Kamberov YG, Pradel J, Wilder EL. (2002). DWnt4 regulates cell movement and focal adhesion kinase during Drosophila ovarian morphogenesis. Dev Cell. 2, 437-48. doi: 10.1016/s1534-5807(02)00142-9.

Davidian A, and Spradling AC (2025). Early female germline development in Xenopus laevis: stem cells, nurse cells and germline cysts. Proc. Natl. Acad. Sci. USA 122, e2522343122. doi: 10.1073/pnas.2522343122.

Deady L.D., Shen W., Mosure S.A., Spradling A.C. and Sun J.J. (2015). Matrix metalloproteinase 2 is required for ovulation and corpus luteum formation in Drosophila. PLoS Genetics 11:e1004989. doi: 10.137.

de Cuevas M, Lee JK, Spradling AC. (1996). α-spectrin is required for germline cell division and differentiation in the Drosophila ovary. Development 122: 3959-3968

DiMario PJ, Mahowald AP. (1987) Female sterile (1) yolkless: a recessive female sterile mutation in Drosophila melanogaster with depressed numbers of coated pits and coated vesicles within the developing oocytes. J Cell Biol 105, 199-206.

Domanitskaya E, Anllo L, Schüpbach T (2014) Phantom, a cytochrome P450 enzyme essential for ecdysone biosynthesis, plays a critical role in the control of border cell migration in Drosophila. Dev Biol 386: 408–418. doi: 10.1016/j.ydbio.2013.12.013.

Drummond-Barbosa D, Spradling AC. (2001). Stem cells and their progeny respond to nutritional changes during Drosophila oogenesis. Dev Biol. 231, 265-78. doi: 10.1006/dbio.2000.0135.

Drummond-Barbosa D. (2019). Local and physiological control of germline stem cell lineages in Drosophila melanogaster. Genetics 213, 9-26.

Dubuke ML, Maniatis S, Shaffer SA, Munson M. (2015). The exocyst subunit Sec6 interacts with assembled exocytic SNARE complexes. J. Biol. Chem. 290, 28245–28256.

Emmons-Bell M & Hariharan I K, (2021). Membrane potential regulates Hedgehog signaling in the *Drosophila* wing imaginal disc. EMBO Reports 22: e51861.

Easwaran S, Van Ligten M, Kui M, Montell DJ (2022). Enhanced germline stem cell longevity in Drosophila diapause. Nat. Commun. 13, 711 (2022).

Forbes Z, Lin H, Ingham P, Spradling AC. (1996). *hedgehog* is required for the proliferation and specification of somatic cells prior to egg chamber formation in Drosophila. Development 122, 1125-1135.

Gall JG. (1996). Views of the the Cell: a pictorial history. American Society for Cell Biology Press.

Gershon E, Issler O, Schroeder M, Kuperman Y, Nevo N, Lazar S, Elbaz M, Dekel N, Chen A. (2025). Mild chronic stress promotes female fertility via the ovarian CRF receptor. Cell Commun Signal. 23, 372. doi: 10.1186/s12964-025-02371-0.

Ghosh G, Das D, Nandi A, De S, Gangappa SN, Prasad M. (2025). Ecdysone regulates phagocytic cell fate of epithelial cells in developing Drosophila eggs. J Cell Biol. 224, e202411073. doi: 10.1083/jcb.202411073.

Godt D, Laski FA. (1995). Mechanisms of cell rearrangement and cell recruitment in Drosophila ovary morphogenesis and the requirement of bric à brac. Development 121, 73-87. doi: 10.1242/dev.121.1.173.

Granados JC, Nigam AK, Bush KT, Jamshidi N, Nigam SK. (2021). A key role for the transporter OAT1 in systemic lipid metabolism. J Biol Chem. 296:100603. doi: 10.1016/j.jbc.2021.100603.

Hagenbuch, B., & Stieger, B. (2013). The SLCO (former SLC21) superfamily of transporters. Molecular Aspects of Medicine 34, 396–412.

Hartenstein V. (2006). The neuroendocrine system of invertebrates: A developmental and evolutionary perspective. J. Endocrinol. 190, 555–570 (2006).

Hatori R, Wood BM, Oliveira Barbosa GO, Kornberg TB (2021) Regulated delivery controls Drosophila Hedgehog, Wingless, and Decapentaplegic signaling. eLife 10:e71744

Heider MR, Munson, M. (2012). Exorcising the exocyst complex. Traffic, 13, 898–907.

Hsu H-J, Bahader M, Lai C-M. (2019). Molecular control of the female germline stem cell niche size in Drosophila. Cell Mol. Life Sci. 76, 4309-17. doi: 10.1007/s00018-019-03223-0.

Hughson BN, Shimell M, O'Connor MB. (2021). AKH Signaling in D. melanogaster Alters Larval Development in a Nutrient-Dependent Manner That Influences Adult Metabolism. Front. Physiol. 12(): 619219.

Irizarry J, Stathopoulos A. FGF signaling supports Drosophila fertility by regulating development of ovarian muscle tissues. (2015). Dev Biol. 404, 1-13. doi: 10.1016/j.ydbio.2015.04.023.

Jenett A, Rubin GM, Ngo TT, Shepherd D, Murphy C, et al. (2012). GAL4-driver line resource for Drosophila neurobiology. Cell Rep. 2: 991–1001. 10.1016/j.celrep.2012.09.011.

Johnson EC, Shafer OT, Trigg JS, Park J, Schooley DA, Dow JA, Taghert PH. (2005). A novel diuretic hormone receptor in Drosophila: evidence for conservation of CGRP signaling. J Exp Biol. 208, 1239-46. doi: 10.1242/jeb.01529.

Kannangara JR, Mirth CK, Warr CG. (2021). Regulation of ecdysone production in Drosophila by neuropeptides and peptide hormones. Open Biol. 11: 200373. https://doi.org/10.1098/rsob.200373.

Karpen GH, Spradling AC. (1992). Analysis of subtelomeric heterochromatin in the Drosophila minichromosme Dp1187 by single-P-element insertional mutagenesis. Genetics 132: 737-53.

King RC, Aggarwal SK, Aggarwal U. (1968). The development of the female Drosophila reproductive system. J Morphol. 124, 143-66. doi: 10.1002/jmor.1051240203.

Knapp E, Sun J. (2017). Steroid signaling in mature follicles is important for Drosophila ovulation. Proc. Natl. Acad. Sci. U.S A., 114, 699-704, 10.1073/pnas.1614383114.

Knapp EM, Li W, Singh V, Sun J. (2020) Nuclear receptor Ftz-f1 promotes follicle maturation and ovulation partly via bHLH/PAS transcription factor Sim eLife 9, e54568

König A, Yatsenko AS, Weiss M, Shcherbata HR (2011) Ecdysteroids affect Drosophila ovarian stem cell niche formation and early germline differentiation. EMBO J 30(8):1549–1562.

Kubrak, O., Koyama, T., Ahrentløv, N., Jensen, L., Malita, A., Naseem, M.T., Lassen, M., Nagy, S., Texada, M.J., Halberg, K.V., Rewitz, K. (2022). The gut hormone Allatostatin C/Somatostatin regulates food intake and metabolic homeostasis under nutrient stress. Nat. Commun. 13(1): 692.

Kurogi Y, Imura E, Mizuno Y, Hoshino R, Nouzova M, Matsuyama S, Mizoguchi A, Kondo S, Tanimoto H, Noriega FG, Niwa R. (2023). Female reproductive dormancy in Drosophila is regulated by DH31-producing neurons projecting into the corpus allatum. Development 150, dev201186. doi: 10.1242/dev.201186.

Lin H, Yue L, Spradling AC. (1994). The Drosophila fusome, a germline specific organelle, contains membrane skeleton proteins, and functions in cyst formation. Development 120: 947-956.

Listenberger LL, Han X, Lewis SE, Cases S, Farese RV, Ory DS, Schaffer JE. (2003). Triglyceride accumulation protects against fatty acid-induced lipotoxicity. Proc. Natl. Acad. Sci. USA, 100, 3077–3082.

Matsuo, N., Nagao, K., Suito, T., Juni, N., Kato, U., Hara, Y., & Umeda, M. (2019). Different mechanisms for selective transport of fatty acids using a single class of lipoprotein in Drosophila. J. Lipid Research, 60, 1199–1211.

Mavridis C, Paspalaki E, Tsatsakis A, Mamoulakis C. (2025). The corticotropin-releasing factor family in the urogenital system (Review). Mol Med Rep. 32, 195. doi: 10.3892/mmr.2025.13560.

Meek S, Hernandez AC, Oliva B, Gallego O. (2024). The exocyst in context. Biohemical Society Transactions 52, 2113-22.

Morgera F, Sallah MR, Dubuke ML, Gandhi P, Brewer DN, Carr CM, Munson M. (2012). Regulation of exocytosis by the exocyst subunit Sec6 and the SM protein Sec1. Mol Biol Cell. 23, 337-46. doi: 10.1091/mbc.E11-08-0670.

Moulton MJ, Barish S, Ralhan I, Chang J, Goodman LD, Harland JG, Marcogliese PC, Johansson JO, Ioannou MS, Bellen HJ. (2021). Neuronal ROS-induced glial lipid droplet formation is altered by loss of Alzheimer's disease-associated genes. Proc Natl Acad Sci U S A. 118, e2112095118. doi:10.1073/pnas.2112095118.

Morris L, Spradling AC. (2011). Long-term live imaging provides new insight into stem cell regulation and germline-soma coordination in the Drosophila ovary. Development 138, 2207-2215.

Morris L, Spradling AC. (2012). Steroid signaling within Drosophila ovarian epithelial cells sex-specifically modulates early germ cell development and meiotic entry. PLoS One 7(10)e46109. doi:10.1371/journal.pone.0046109.

Nath DK, Dhakal S, Lee S. (2025) TRPγ regulates lipid metabolism through Dh44 neuroendocrine cells eLife 13:RP99258 https://doi.org/10.7554/eLife.99258.3

Nguyen, T. B., Louie, S. M., Daniele, J. R., Tran, Q., Dillin, A., Zoncu, R., Nomura, D. K., & Olzmann, J. A. (2017). DGAT1-dependent lipid droplet biogenesis protects mitochondrial function during starvation-induced autophagy. Dev Cell 42, 9–21.

Obniski R, Sieber M, Spradling AC. (2018). Dietary Lipids Modulate Notch Signaling and Influence Adult Intestinal Development and Metabolism in Drosophila. Dev Cell 47, 98-111.e5. doi: 10.1016/j.devcel.2018.08.013.

Okamoto N, Viswanatha R, Bittar R, Li Z, Haga-Yamanaka S, Perrimon N, Yamanaka N. (2018). A Membrane Transporter Is Required for Steroid Hormone Uptake in Drosophila. Dev. Cell 47, 294-305.

Olzmann JA, Carvalho P. (2019). The biogenesis and functions of lipid droplets. Nature Reviews Molecular Cell Biology. 20, 137–155.

Palm W, Sampaio JL, Brankatschk M, Carvalho, M, Mahmoud A, Shevchenko A, Eaton S. (2012). Lipoproteins in Drosophila melanogaster-- Assembly, function, and influence on tissue lipid composition. PLoS Genetics 8, e1002828.

Parra-Peralbo, E., and Culi, J. (2011). Drosophila lipophorin receptors mediate the uptake of neutral lipids in oocytes and imaginal disc cells by an endocytosis-independent mechanism. PLoS Genet. 7, e1001297.

Pathak M, and Spradling AC (2026). Mouse germline cysts contain a fusome-like structure that mediates oocyte development. eLife 15, RP109358 https://doi.org/10.7554/eLife.109358.

Petrella LN, Smith-Leiker T, Cooley L. (2007). The Ovhts polyprotein is cleaved to produce fusome and ring canal proteins required for Drosophila oogenesis. Development 134, 703-12. doi: 10.1242/dev.02766.

Petryk A, Warren JT, Marqués G, Jarcho MP, Gilbert LI, Kahler J, Parvy JP, Li Y, Dauphin-Villemant C, O'Connor MB. (2003). Shade is the Drosophila P450 enzyme that mediates the hydroxylation of ecdysone to the steroid insect molting hormone 20-hydroxyecdysone. Proc Natl Acad Sci U S A. 100, 13773-8. doi: 10.1073/pnas.2336088100.

Porter JA, Young KE, Beachy PA. (1996). Cholesterol modification of Hedgehog signaling proteins in animal development. Science 274, 255–259.

Rambold, A. S., Cohen, S. L., & Lippincott-Schwartz, J. (2015). Fatty acid trafficking in starved cells: Regulation by lipid droplet lipolysis, autophagy, and mitochondrial fusion dynamics. Developmental Cell, 32, 678–692.

Ramachandran P, Budnik V. (2010). Fm1-43 labeling of Drosophila larval neuromuscular junctions. Cold Spring Harb Protoc. 2010 Aug 1;2010(8):pdb.prot5471. doi: 10.1101/pdb.prot5471.

Sahut-Barnola I, Godt D, Laski FA, Couderc JL. (1995). Drosophila ovary morphogenesis: analysis of terminal filament formation and identification of a gene required for this process. Dev Biol. 170, 127-35. doi: 10.1006/dbio.1995.1201.

Sarikaya DP, Belay AA, Ahuja A, Dorta A, Green DA 2nd, Extavour CG. (2012). The roles of cell size and cell number in determining ovariole number in Drosophila. Dev Biol. 363, 279-89. doi: 10.1016/j.ydbio.2011.12.017.

Scanlan JL, Robin C, Mirth CK. (2023) Rethinking the ecdysteroid source during Drosophila pupal-adult development. Insect Biochem Mol Biol. 152:103891. doi: 10.1016/ j.ibmb.2022.103891.

Sieber MH, Spradling AC. (2015). Steroid Signaling Establishes a Female Metabolic State and Regulates SREBP to Control Oocyte Lipid Accumulation. Curr Biol. 25, 993-1004. doi: 10.1016/j.cub.2015.02.019.

Slaidina M, Banisch TU, Gupta S, Lehmann R. (2020). A single-cell atlas of the developing *Drosophila* ovary identifies follicle stem cell progenitors. Genes Dev. 34, 239-249. doi: 10.1101/gad.330464.119.

Slaidina M, Gupta S, Banisch TU, Lehmann R. (2021). A single-cell atlas reveals unanticipated cell type complexity in *Drosophila* ovaries. Genome Res. 2021 31, 1938-1951. doi: 10.1101/gr.274340.120.

Song X, Call GB, Kirilly D, Xie T. (2007). Notch signaling controls germline stem cell niche formation in the Drosophila ovary. Development. 134, 1071-80. doi: 10.1242/dev.003392.

Spradling A, Pathak M, Davidian A, Maurya B (Bhawana Maurya), Tiwari A, Yin Q, Fu Y, Mao A.(2025) Hypothesis: Germline rejuvenation during meiosis underlies animal oogenesis. Dev. Biology 527, 65-76. doi: 10.1016/j.ydbio.2025.08.002.

Sun J, Smith L, Armento A, Deng WM (2008) Regulation of the endocycle/gene amplification switch by Notch and ecdysone signaling. J Cell Biol 182, 885–896

Svoboda M, Mungenast F, Gleiss A, Vergote I, Vanderstichele A, Sehouli J, Braicu E, Mahner S, Jäger W, Mechtcheriakova D, Cacsire-Tong D, Zeillinger R, Thalhammer T, Pils D. (2018). Clinical Significance of Organic Anion Transporting Polypeptide Gene Expression in

High-Grade Serous Ovarian Cancer. Front Pharmacol. 9, 842. doi: 10.3389/fphar.2018.00842.

Terashima J, Takaki K, Sakurai S, Bownes M (2005) Nutritional status affects 20-hydroxyecdysone concentration and progression of oogenesis in Drosophila melanogaster. J Endocrinol 187(1):69–79.

Thomalla JM, Giedt MS, White RP, Wipf IJ, Shipley A, Chen M, Welte MA, Tootle TL. (2025). The lipid droplet protein Jabba promotes actin remodeling downstream of prostaglandin signaling during *Drosophila* oogenesis. Mol Biol Cell. 36, ar105. doi: 10.1091/mbc.E25-05-0218.

Torrie, L.S., Radford, J.C., Southall, T.D., Kean, L., Dinsmore, A.J., Davies, S.A., Dow, J.A. (2004). Resolution of the insect ouabain paradox. Proc. Natl. Acad. Sci. U.S.A. 101, 13689-13693.

Walther, T. C., & Farese, R. V. (2012). Lipid droplets and cellular lipid metabolism. Annual Review of Cell and Developmental Biology. *28.* 1–26.

Welte MA. (2015). As the fat flies: The dynamic lipid droplets of Drosophila embryos. Biochim Biophys Acta. 1851, 1156-85. doi: 10.1016/j.bbalip.2015.04.002.

Welte, M. A., & Gould, A. P. (2017). Lipid droplet functions beyond energy storage. Biochimica et Biophysica Acta (BBA) – Molecular and Cell Biology of Lipids. 1862(10). 1260–1272.

Yoshida S. (2020). From cyst to tubule: innovations in vertebrate spermatogenesis. WIREs Dev Biol 2016, 5:119–131. doi: 10.1002/wdev.204

Zhang C, Daubnerova I, Jang YH, Kondo S, Žitňan D, Kim YJ. (2021). The neuropeptide allatostatin C from clock-associated DN1p neurons generates the circadian rhythm for oogenesis. Proc Natl Acad Sci U S A. 118, e2016878118. doi: 10.1073/pnas.2016878118.

Zhu C-H, Xie T. (2003). Clonal expansion of ovarian germline stem cells during niche formation in Drosophila. Developoment 130, 2579-2586.

Zhu H., Ludington W., Spradling A.C. (2024). Cellular and molecular organization of the Drosophila foregut. Proc. Natl. Acad. Sci, USA 121(11):e2318760121. doi: 10.1073/pnas.2318760121.

FIGURE LEGENDS

Figure 1: Identification of terminal filament genes and germarium lipid droplets

(A) Schematic diagram of the germarium, highlighting the terminal filament (TF), cap cells (cap) and anterior escort (EC) cells that maintain a niche for 2-3 germline stem cells (GSCs). Two follicle stem cells (FSCs) reside singly in separate small niches maintained by posterior ECs on each side of the germarium at the junction or region 2a and 2b, two of four germarium regions. **(B-F)** TF and germarium from enhancer trap lines in B) Oatp30B (PZ00078); C) anti-Atpα (a5) reveals strong enrichment of Na□/K□-ATPase in terminal filament cells; D) Dh44-R2 (PZ00275); E) cenB1A (PZ03627) and F) AstC-R2 (R11A12) (scale bar=5μm). **(G-I)** Germarium and first follicle stained with (G) BODIPY 493/503, (H) Nile Red, and (I) LipidTOX to visualize neutral lipids. Lipid droplets (LDs), marked by these neutral lipid stains, are distributed throughout the germarium. **(J)** Quantification of lipid droplet number in distinct cell types of the germarium, large LDs are present in germ cells and at lesser numbers in follicle cells (n, represents number of examined germarium). **(K)** A rare EM cross section of an anterior germarium showing the presence of abundant small vesicles (arrow), some in rows, in the posterior TF cell cytoplasm, an adjacent cap cell (CC) and nearby ECs and GSCs, and surrounding sheath (SH). bar: 2μ.

Figure 2: Oatp74D and Oatp30B mediated transport in the terminal filament regulates cyst development.

(A) Germarium tip from a *bab1-GAL4* driven *nls:GFP* ovary stained with GFP and DAPI which marks the TF and CC cells. **(B)** LDs labeled with BODIPY 493/503 and fusome with Hts in control germarium. **(C-D)** Knockdown (KD) of Organic anion transporting polypeptide 74D (*Oatp74D*) in TF and CC was achieved using *tub-GAL80^{ts}, bab1-GAL4*, with RNAi induced at 29 °C from day 1 and analyzed on day 3. Spectrosome-like structures and shortened fusomes were observed in region 2A compared to control germaria (B). **(E-F)** Knockdown (KD) of Oatp74D at the pupal stage (48 hours after puparium formation, APF) results in defective lens-shaped cysts in region 2b. **(G)** Quantification shows an increased frequency of short fusomes or spectrosome-like structures in adult Oatp74D KD germaria. **(H)** Graph depicting a reduction in lipid droplet (LD) number upon *Oatp74D* KD at pupal and adult stage (n=18). **(I)** *Oatp30B* KD in the TF was carried out as for *Oatp7D*. LDs were strongly reduced, moreover, KD caused a block in cyst production indicated by a large increase in germ cells containing spectrosomes**. (J)** Quantification showing increase in number of spectrosome till region2A in *Oatp30B* knockdown compared to control. **(K-R)** *Oatp30B* was knocked down using *bab-GAL4, tub-GAL80^{ts}* starting on day 1 of adult eclosion, and lipid droplets were assessed at 12-hour intervals. A noticeable reduction in lipid droplet number was observed from 24 hours onwards, with a gradual decrease over time. **(S)** Graph representing quantification of lipid droplet numbers in the germarium over time, showing a decline from 24 to 36 hours, followed by a stable, low number of lipid droplets at later time points. (**T**) Graph showing reduced lipid droplet volume in the germarium from 24 hour onwards following *Oatp30B* knockdown compared to control. Sample sizes are indicated in

the graph (n=14). Statistical significance was determined using an unpaired two-tailed t-test (*P < 0.05, **P < 0.01, ***P < 0.001).

Figure 3: Terminal filament specific knockdowns of Oatp30B and LpR2 differentially affect Hedgehog signaling, lipid droplets and cyst formation.

(A, A') Hedgehog (Hh) staining shows robust expression in TF and CC of control germarium. **(B, B')** *Oatp30B* knockdown with *bab1-GAL4, tub-GAL80^{ts}* shifted at 29° C at day1 and analyzed at day2, dramatically reduced Hh expression in TF and CC cells. **(C)** Quantification of Hh fluorescence intensity in the TF confirms a reduction following *Oatp30B* depletion (n=14). **(D)** Quantification of spectrosome reveals an increase in Atpα knockdown germarium compared to control. **(E–F)** *Atpα* knockdown using the same driver as for *Oatp30B*, with RNAi induced at 29 °C from day 1 and analyzed on day 3, shows increased spectrosome extending through region 2A of the germarium (F) compared to control (E). **(G)** LpR2 knockdown in terminal filament and cap cells on adult day1and analyzed on day3, leads to a reduction in lipid droplet number within the germarium, a smaller region 2A with less-branched fusomes, and defects in cyst development. **(H)** Graph showing the reduction in lipid droplet volume within germ cells over time (0–48 h) following LpR2 knockdown in terminal filament and cap cells, lipid reduction begins around 12 h post-knockdown. **(I–J)** Hts and lipid droplet staining in terminal filament and cap cells shows Hts aggregates at day 1 that disappear by day 3. **(K)** Quantification of Hts aggregates in TF and CC cells from day 1 to day 5 (n=15). (n, represents number of samples analyzed, statistical significance *P < 0.05, **P < 0.01, ***P < 0.001)

Figure 4: Terminal filament delivers lipids to LDs of germ cells through exocyst-dependent vesicle trafficking.

(A) BODIPY 493/503 staining of control germarium shows normal lipid droplet (LD) distribution at 4d post-eclosion. (temperature shifted to 29□°C, at late pupal stage). **(B)** Conditional knockdown of *Sec6* in terminal filament cells using the *bab1-GAL4, tub-Gal80^{ts}* shows strong depletion of lipid droplets by day 4 post-eclosion. (temperature shifted to 29□°C, at late pupal stage). **(A')** Higher magnification of control germarium (A) showing that LDs are nearly absent under normal conditions in TF and cap cells. **(B')** Higher magnification of Sec6 KD germarium (B), showing accumulation of enlarged LDs in TF and cap cells, suggesting impaired lipid export due to disrupted exocytosis. (**C**) Control ovariole with normal cyst and developing follicles. (**D**) *Sec6* KD showing defective cyst and follicle development marked with arrow. **(E)** Quantification of LD number in control vs. *Sec6* knockdown, showing a significant decrease in LD number. **(F)** Quantitative analysis reveals a significant increase in LD number and size within the TF following *Sec6* knockdown. (**G, G'**) *hh-GAL4* driven *nls:GFP* marks TF, CC and EC (**H,I**) *hh-GAL4* driven *Sec6* KD leads to accumulation of LDs only in TF and CC cells, not in escort cells, with loss of LDs from the germarium, compared to control **(H)**. (**J**) Graph represents significant reduction of LDs from hh-GAL4 driven Sec6 KD germarium. (**K, K'**) *c587-GAL4* driven GFP marks escort cells in germarium. (**M**) *Sec6* knockdown in escort cells driven by *c587-GAL4* disrupts cyst and follicle formation, but LD levels in germ cells remain largely unaffected, compared to control (**N**). **(N)** Quantification of LD signal in germ cells shows no significant difference between control and escort cell specific *Sec6* knockdown, supporting a limited role for escort cells in lipid transport. (n, represents number of samples analyzed, Unpaired two-tailed t-test, *P < 0.05, **P < 0.01, ***P < 0.001).

Figure 5: Kinetics of Sec6-dependent lipid transfer from terminal filament to the germarium.

(**A**) Control germarium showing normal distribution of lipid droplets throughout the germarium. **(B-K)** LD staining (BODIPY 493/503) of germarium at 6-hour interval from 0 to 72 hours post-eclosion following *Sec6* knockdown using *bab1-GAL4, tub-GAL80^{ts}*, with temperature shift to 29 °C. LDs accumulate within the TF from 12 hours, while their levels are markedly reduced in germ cells strating from 18hours. **(L)** LD quantification in the germarium showed consistent depletion following *Sec6* knockdown from 18 hours and onwards relative to controls (n=10, individual data point shown in graph). (**M**) Quantification shows volume of lipid in LDs of germarium starts to decline from ~18 hour onwards and by 30-36 hours showed complete depletion compared to control (n=10, individual data point shown in graph). **(N)** Quantification of LD content in the TF following *Sec6* knockdown confirms significantly elevated lipid levels across time points (n=10). **(O)** Quantification of lipid volume in TF cells shows a steady increase from 12 hours to 48 hours in Sec6 knockdown compared with control (n=10). (**P**) Graph represents LD count within different regions of germarium in *Sec6* knockdown, were significant number of LD persists in R1 till 24, as compared to R2a, R2b, R3 with sever reduction from 24hours (n=24). (**Q**) Quantification shows defective 16 cell cyst formation from 36 hours compared to control (n=24). n represents number of samples analyzed, Statistical significance, Unpaired two-tailed t-test, *P < 0.05, **P < 0.01, ***P < 0.001).

Figure 6: Lipid droplets protect early germ cells from mitochondrial ROS accumulation.

(A) Control germarium showing close association of lipid droplets (BODIPY 493/503) with mitochondria (Cyto C). **(B–C)** Control (B) and germ cell-specific *ACC* knockdown (C) ovaries (using *nanos-GAL4*), showing severe loss of LDs upon depletion of the lipogenic enzyme Acetyl-CoA Carboxylase. **(D)** Quantification of LD levels in germ cells shows a significant reduction following *ACC* knockdown. **(E–G)** MitoSOX staining reveals elevated mitochondrial ROS in *ACC* knockdown (F) and TF-specific *Sec6* knockdown (G), compared to control (E). **(H-J)** DHE staining detects increased ROS levels in *ACC* knockdown (I) and TF-*Sec6* knockdown (J) germaria relative to control (H). **(K)** Quantification of MitoSOX signal intensity shows significant ROS increase in both *ACC*- and *Sec6*-depleted germaria (n=18). **(L)** Quantification of DHE signal intensity confirms significantly elevated ROS in both experimental conditions, supporting a protective role for LDs against oxidative stress (n=23). (n, represents number of samples analyzed, Unpaired two-tailed t-test *P < 0.05, **P < 0.01, ***P < 0.001).

Figure 7: Model for terminal filament uptake, intercellular transport and delivery of cargos to germarium.

(A) Terminal filament (TF) cells actively incorporate molecules from the hemolymph via transporter (Oatp74D, Oatp30B) and receptor (LpR2), process and package them, and deliver the resulting cargo including lipids, and organic solutes to ovariolar germ cells via vesicle-mediated trafficking through transcytosis. **(B)** Terminal filament mediated transport (hormone and lipophilic molecule transport shown in blue) regulates follicle development in an ovariole-specific manner within the epithelial sheath.

SUPPLEMENTAL FIGURE LEGENDS

Figure S1: LpR2 knockdown reduces lipid droplets and causes cyst defects in the germarium.

(A-H) Lipoprotein receptor (*LpR2*) KD in the TF and CC using *bab1-GAL4, tub-GAL80^{ts}* with RNAi induced at 29 °C at day1, and analyzed over 6-hour time interval. LD number depletion within the germarium starts from 12 hour onwards, along with less branched fusome (arrow) and defect in cyst development (arrowhead). **(I)** Control germarium showing lipid distribution throughout the germarium. **(I)** Control germarium showing lipid droplet distribution and Hts-labeled fusome. **(J)** Quantification of lipid droplets in the germarium reveals a gradual decrease by 12 h, a pronounced reduction from 24 h onward, and a stable, low number at later time points. (Sample sizes are indicated in the graph.; unpaired two-tailed t-test: $P < 0.05$, $P < 0.01$, $P < 0.001$).

Figure S2: Active exocytosis in terminal filament and cap cells with lipid droplet accumulation.

(A) Egg laying assay showing a significant reduction in the number of eggs produced per female per day following *Sec6* knockdown with *bab1-GAL4* (n=3). **(B)** FM1-43 dye staining in control germarium shows strong signal in TF and cap cells, indicative of active vesicle trafficking and membrane recycling. **(C)** FM1-43 staining is markedly reduced in TF and cap cells following *Sec6* knockdown, suggesting impaired exocytosis. **(D)** Quantitative analysis of FM1-43 fluorescence intensity confirms a significant reduction in TF/cap cells in *Sec6* knockdown samples compared to controls (n=12). (**E, E'**) LDs stained with nile red in control germarium. (**F, F'**) Depletion of nile red positive LDs in germarium of Sec6 knockdown in TF and CC, along

with accumulation of LDs in TF and CC cells. (**G**)Graph represents reduction of LDs in Sec6 knockdown (n=15). N represents number of samples analyzed, statistical significance *P < 0.05, **P < 0.01, ***P < 0.001.

Figure S3: Exocyst complex component knockdown shows lipid droplet depletion from germarium.

(**A**)Control showing normal LDs distribution **(B-F)** Conditional knockdown of exocyst genes (*Sec10, Sec15, Sec5, Exo70, Exo84*) , showing LD depletion from germ cell of germarium (temperature shiftedat day1 of adult eclosion, dissected on day 2). LaminC (TF marker), BODIPY (LDs), and DAPI (nuclei). (**G**) Quantification of LD in different exocyst component knockdown with reduction in LD throughout the germarium (n=19). (n, represents number of samples analyzed, statistical significance *P < 0.05, **P < 0.01, ***P < 0.001).

Figure S4: Terminal filament and cap cell derived cargo transport is essential for fusome maintenance and cyst development.

(A, A') Control germarium showing LD (BODIPY) distribution and fusome (Hts)**. (B-E)** Hts and BODIPY stain in *Sec6* knockdown germarium at day1,2,3, and 4. LD and Hts accumulation starts from day1 in TF and CC cells, with LD depletion in germ cells of germarium, along with defective fusome and cyst from day2 onwards. **(B'–E')** Hts staining shows progressive accumulation of Hts-positive cytoskeletal aggregates in TF cells from day 1 to 4, these aggregates are absent in control germarium **(A')**. (**I-J)** Quantification shows increase in number and size of Hts aggregate per TF at days 1, 2,3 and 4 post-eclosion in *Sec6* knockdown (n=15). **(K)** Quantification show that *Sec6*-depleted TF cells lead to reduced spectrosome volume in

GSCs compared to control (n=15). (n, represents number of samples analyzed, statistical significance *P < 0.05, **P < 0.01, ***P < 0.001)

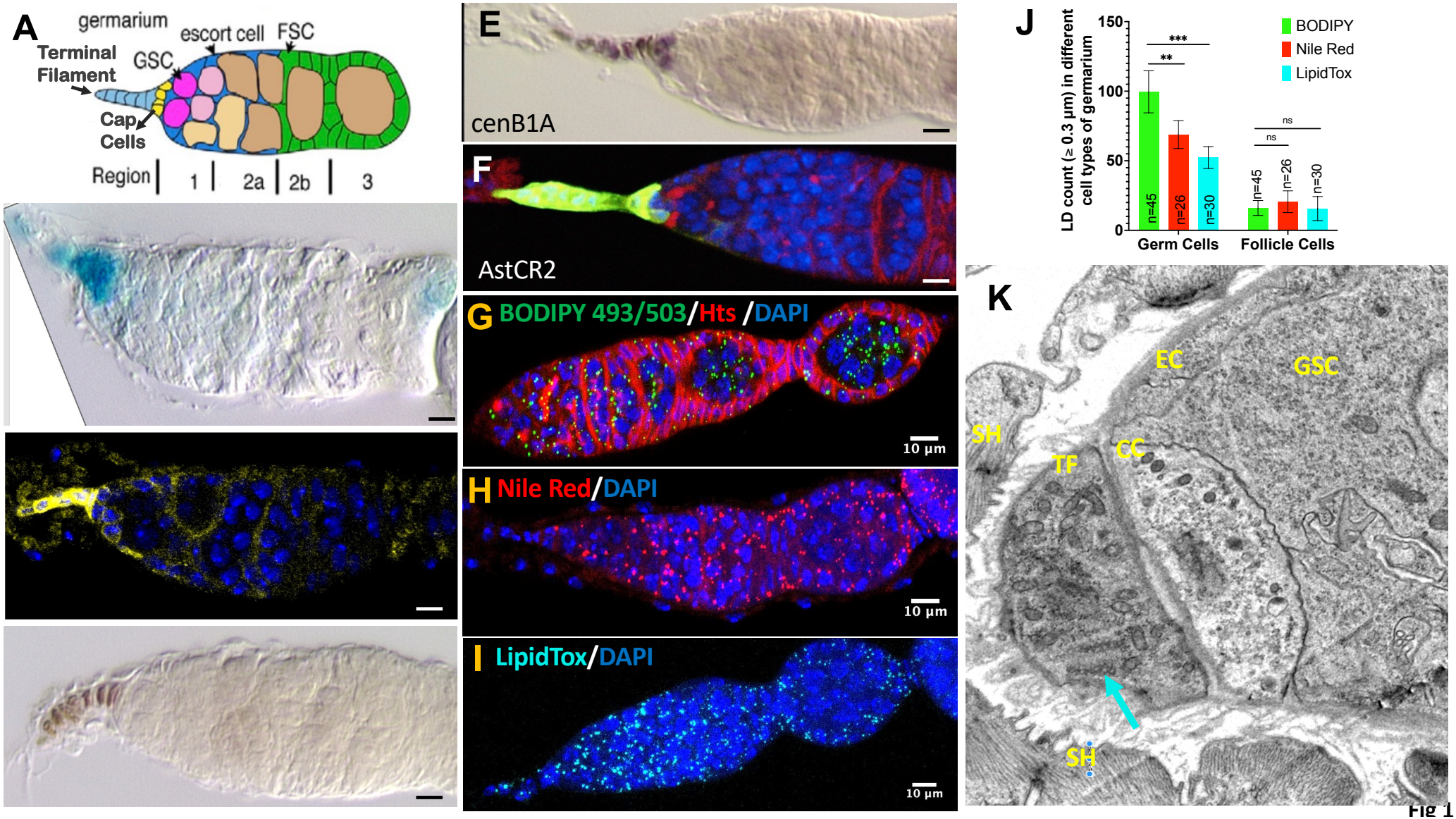
A
germarium
escort cell
FSC
Terminal Filament
GSC
Cap Cells
Region
1
2a
2b
3
E
cenB1A
F
AstCR2
G BODIPY 493/503/Hts /DAPI
10 µm
H Nile Red/DAPI
10 µm
I LipidTox/DAPI
10 µm
J
LD count (≥ 0.3 µm) in different cell types of germarium
150
100
50
0
***
**
ns
ns
n=45
n=26
n=30
n=45
n=26
n=30
Germ Cells
Follicle Cells
BODIPY
Nile Red
LipidTox
K
EC
GSC
SH
TF
CC
SH

Fig 1

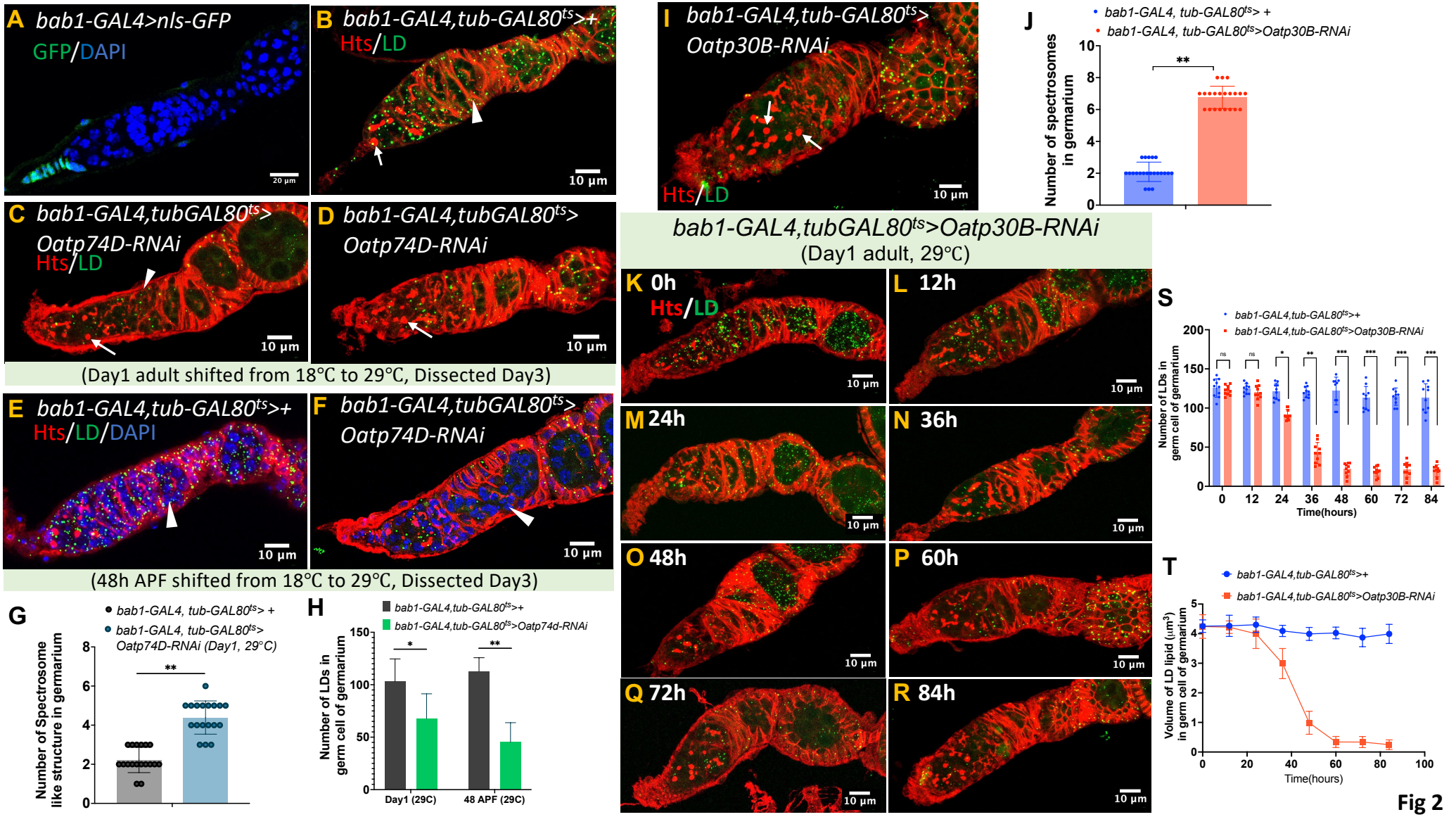
A bab1-GAL4>nls-GFP
GFP/DAPI
20 µm
B bab1-GAL4,tub-GAL80ts>+
Hts/LD
10 µm
C bab1-GAL4,tubGAL80ts>
Oatp74D-RNAi
Hts/LD
10 µm
D bab1-GAL4,tubGAL80ts>
Oatp74D-RNAi
10 µm
(Day1 adult shifted from 18°C to 29°C, Dissected Day3)
E bab1-GAL4,tub-GAL80ts>+
Hts/LD/DAPI
10 µm
F bab1-GAL4,tubGAL80ts>
Oatp74D-RNAi
10 µm
(48h APF shifted from 18°C to 29°C, Dissected Day3)
G
bab1-GAL4, tub-GAL80ts> +
bab1-GAL4, tub-GAL80ts>
Oatp74D-RNAi (Day1, 29°C)
Number of Spectrosome like structure in germarium
**
H
bab1-GAL4,tub-GAL80ts>+
bab1-GAL4,tub-GAL80ts>Oatp74d-RNAi
Number of LDs in germ cell of germarium
Day1 (29C)
48 APF (29C)
I bab1-GAL4,tub-GAL80ts>
Oatp30B-RNAi
Hts/LD
10 µm
J
bab1-GAL4, tub-GAL80ts> +
bab1-GAL4, tub-GAL80ts>Oatp30B-RNAi
Number of spectrosomes in germarium
**
bab1-GAL4,tubGAL80ts>Oatp30B-RNAi
(Day1 adult, 29°C)
K 0h
Hts/LD
L 12h
M 24h
N 36h
O 48h
P 60h
Q 72h
R 84h
S
bab1-GAL4,tub-GAL80ts>+
bab1-GAL4,tub-GAL80ts>Oatp30B-RNAi
Number of LDs in germ cell of germarium
Time(hours)
T
bab1-GAL4,tub-GAL80ts>+
bab1-GAL4,tub-GAL80ts>Oatp30B-RNAi
Volume of LD lipid (µm³) in germ cell of germarium
Time(hours)

Fig 2

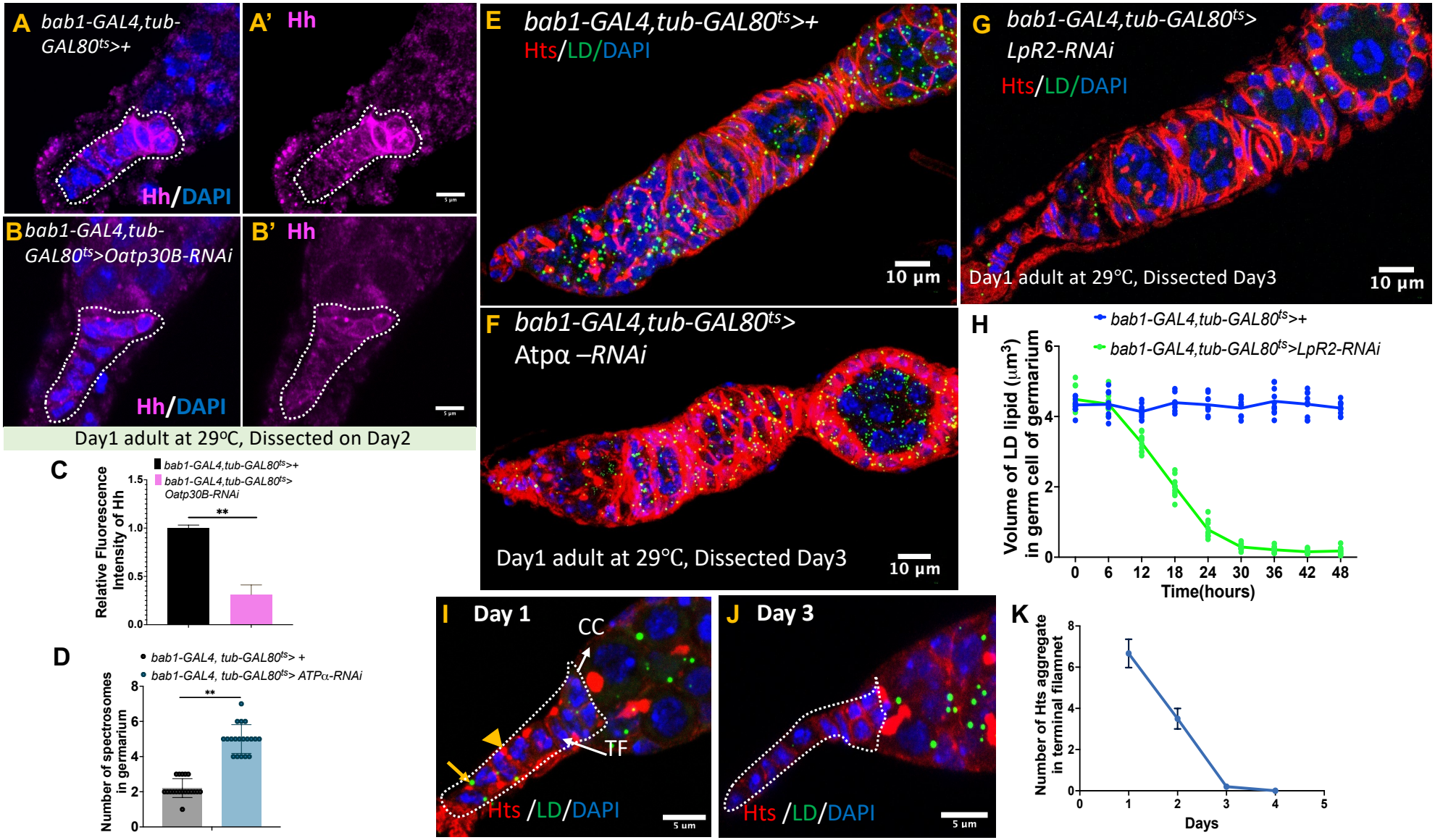
A bab1-GAL4,tub-GAL80ts>+
Hh/DAPI
A' Hh
B bab1-GAL4,tub-GAL80ts>Oatp30B-RNAi
Hh/DAPI
B' Hh
Day1 adult at 29ºC, Dissected on Day2
C
bab1-GAL4,tub-GAL80ts>+
bab1-GAL4,tub-GAL80ts> Oatp30B-RNAi
Relative Fluorescence Intensity of Hh
**
D
bab1-GAL4, tub-GAL80ts> +
bab1-GAL4, tub-GAL80ts> ATPα-RNAi
Number of spectrosomes in germarium
**
E bab1-GAL4,tub-GAL80ts>+
Hts/LD/DAPI
10 µm
F bab1-GAL4,tub-GAL80ts> Atpα –RNAi
Day1 adult at 29°C, Dissected Day3
10 µm
G bab1-GAL4,tub-GAL80ts> LpR2-RNAi
Hts/LD/DAPI
Day1 adult at 29°C, Dissected Day3
10 µm
H
bab1-GAL4,tub-GAL80ts>+
bab1-GAL4,tub-GAL80ts>LpR2-RNAi
Volume of LD lipid (µm3) in germ cell of germarium
Time(hours)
I Day 1
CC
TF
Hts /LD/DAPI
5 um
J Day 3
Hts /LD/DAPI
5 um
K
Number of Hts aggregate in terminal filamnet
Days

Fig 3

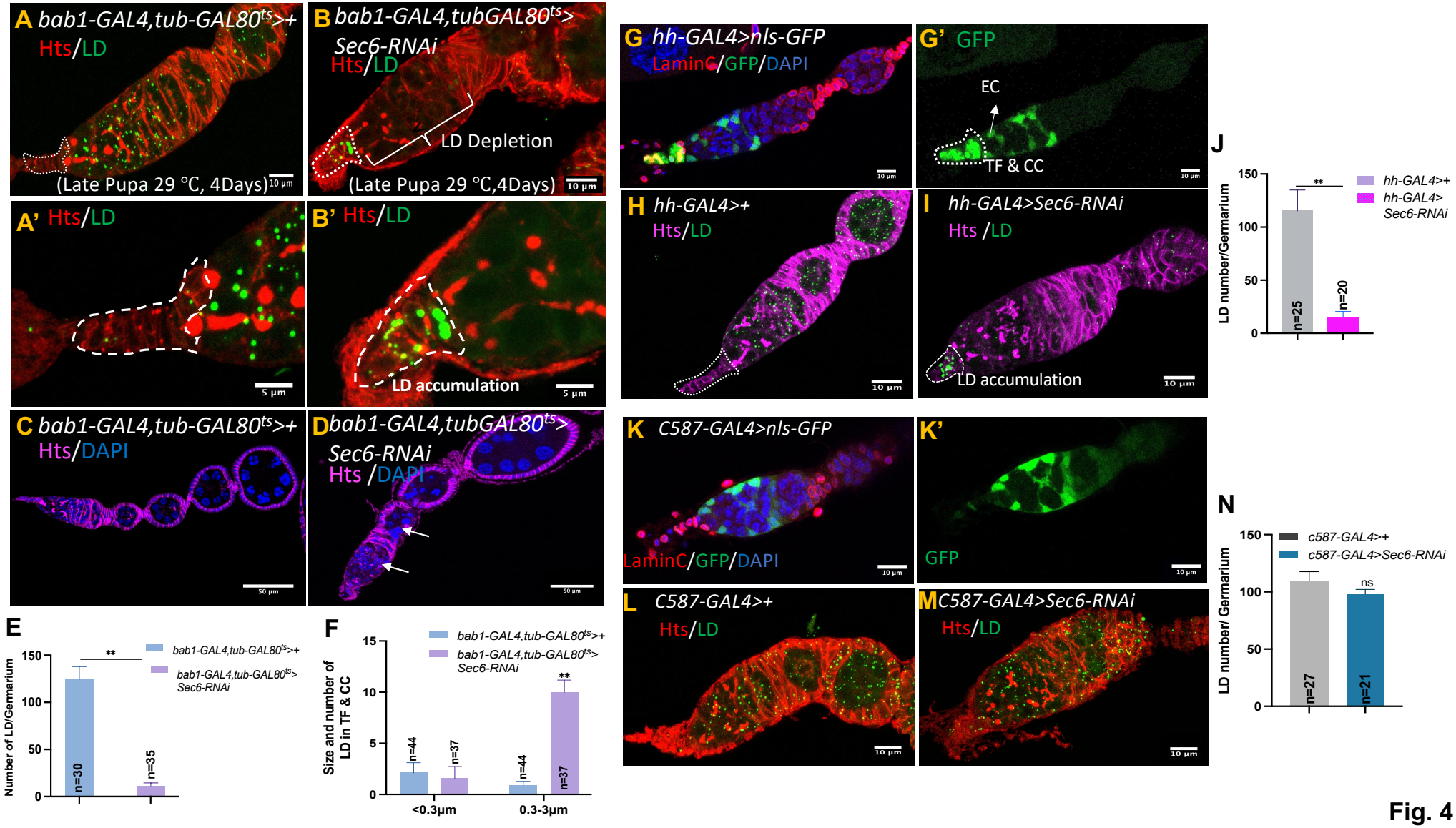
A bab1-GAL4,tub-GAL80ts>+
Hts/LD
(Late Pupa 29 °C, 4Days)
10 µm
B bab1-GAL4,tubGAL80ts>
Sec6-RNAi
Hts/LD
LD Depletion
(Late Pupa 29 °C,4Days)
10 µm
A' Hts/LD
5 µm
B' Hts/LD
LD accumulation
5 µm
C bab1-GAL4,tub-GAL80ts>+
Hts/DAPI
50 µm
D bab1-GAL4,tubGAL80ts>
Sec6-RNAi
Hts /DAPI
50 µm
E
Number of LD/Germarium
150
100
50
0
**
bab1-GAL4,tub-GAL80ts>+
bab1-GAL4,tub-GAL80ts>
Sec6-RNAi
n=30
n=35
F
Size and number of
LD in TF & CC
15
10
5
0
bab1-GAL4,tub-GAL80ts>+
bab1-GAL4,tub-GAL80ts>
Sec6-RNAi
**
n=44
n=37
n=44
n=37
<0.3µm
0.3-3µm
G hh-GAL4>nls-GFP
LaminC/GFP/DAPI
10 µm
G' GFP
EC
TF & CC
10 µm
H hh-GAL4>+
Hts/LD
10 µm
I hh-GAL4>Sec6-RNAi
Hts /LD
LD accumulation
10 µm
J
LD number/Germarium
150
100
50
0
**
hh-GAL4>+
hh-GAL4>
Sec6-RNAi
n=25
n=20
K C587-GAL4>nls-GFP
LaminC/GFP/DAPI
10 µm
K'
GFP
10 µm
L C587-GAL4>+
Hts/LD
10 µm
M C587-GAL4>Sec6-RNAi
Hts/LD
10 µm
N
LD number/ Germarium
150
100
50
0
c587-GAL4>+
c587-GAL4>Sec6-RNAi
ns
n=27
n=21

Fig. 4

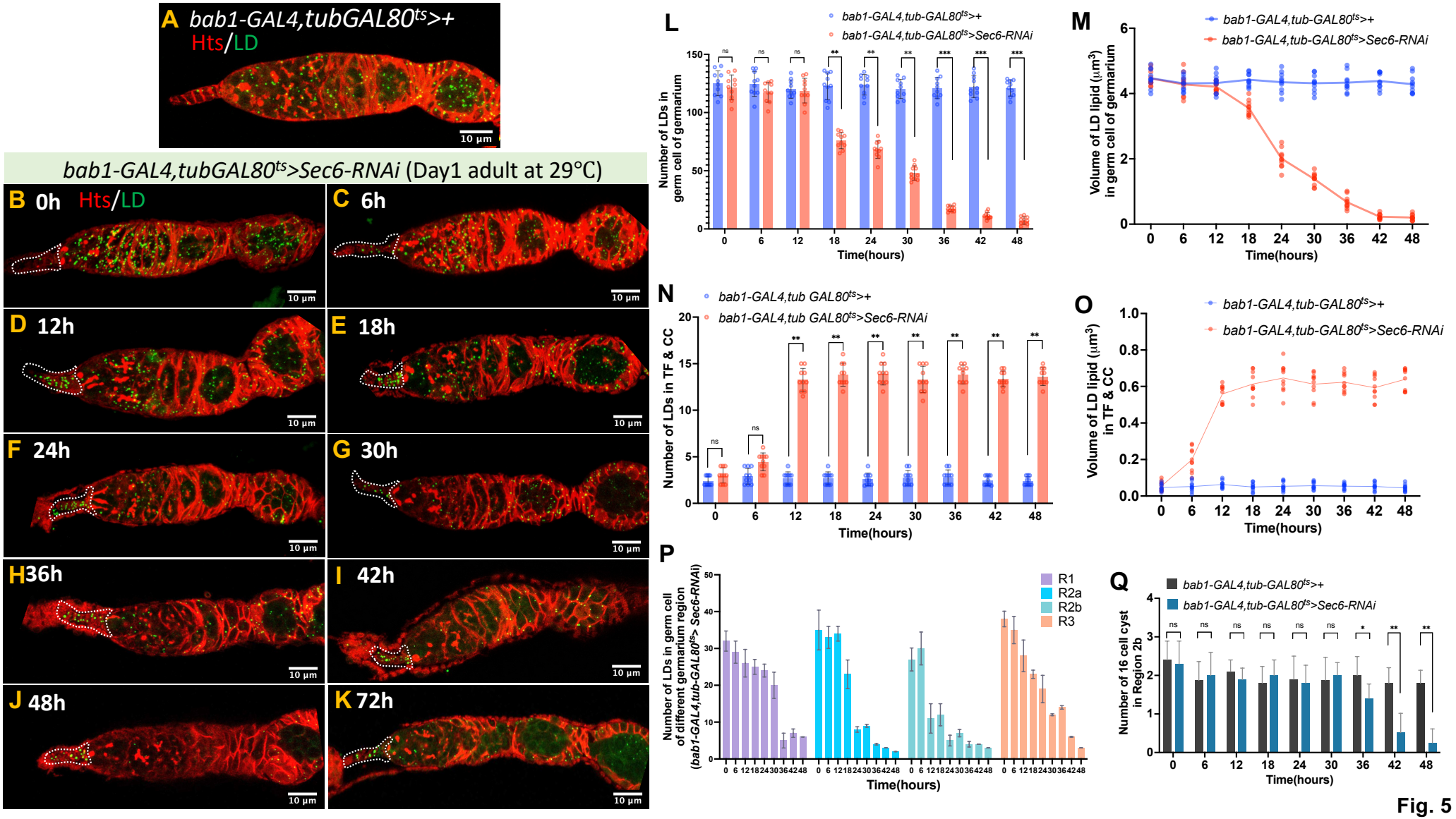
A bab1-GAL4,tubGAL80ts>+
Hts/LD
10 μm
bab1-GAL4,tubGAL80ts>Sec6-RNAi (Day1 adult at 29°C)
B 0h Hts/LD
C 6h
D 12h
E 18h
F 24h
G 30h
H36h
I 42h
J 48h
K 72h
L
bab1-GAL4,tub-GAL80ts>+
bab1-GAL4,tub-GAL80ts>Sec6-RNAi
Number of LDs in germ cell of germarium
Time(hours)
M
Volume of LD lipid (μm3) in germ cell of germarium
N
bab1-GAL4,tub GAL80ts>+
bab1-GAL4,tub GAL80ts>Sec6-RNAi
Number of LDs in TF & CC
O
Volume of LD lipid (μm3) in TF & CC
P
R1
R2a
R2b
R3
Number of LDs in germ cell of different germarium region (bab1-GAL4,tub-GAL80ts> Sec6-RNAi)
Q
Number of 16 cell cyst in Region 2b

Fig. 5

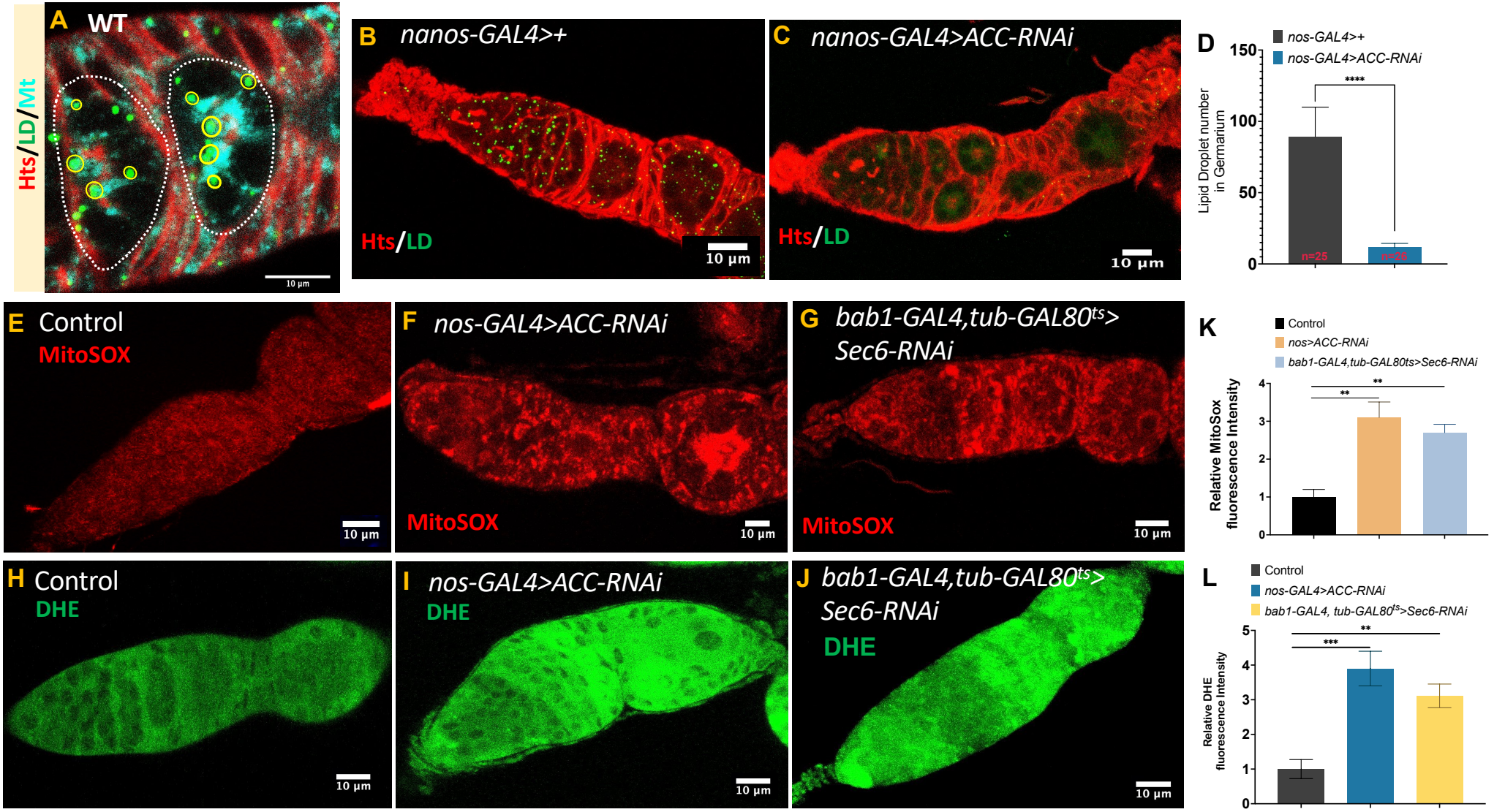
A WT
Hts/LD/Mt
10 µm
B nanos-GAL4>+
Hts/LD
10 µm
C nanos-GAL4>ACC-RNAi
Hts/LD
10 µm
D
nos-GAL4>+
nos-GAL4>ACC-RNAi
Lipid Droplet number in Germarium
150
100
50
0
****
n=25
n=26
E Control
MitoSOX
10 µm
F nos-GAL4>ACC-RNAi
MitoSOX
10 µm
G bab1-GAL4,tub-GAL80ts> Sec6-RNAi
MitoSOX
10 µm
K
Control
nos>ACC-RNAi
bab1-GAL4,tub-GAL80ts>Sec6-RNAi
Relative MitoSox fluorescence Intensity
4
3
2
1
0
**
**
H Control
DHE
10 µm
I nos-GAL4>ACC-RNAi
DHE
10 µm
J bab1-GAL4,tub-GAL80ts> Sec6-RNAi
DHE
10 µm
L
Control
nos-GAL4>ACC-RNAi
bab1-GAL4, tub-GAL80ts>Sec6-RNAi
Relative DHE fluorescence Intensity
5
4
3
2
1
0
**
***

Fig 6

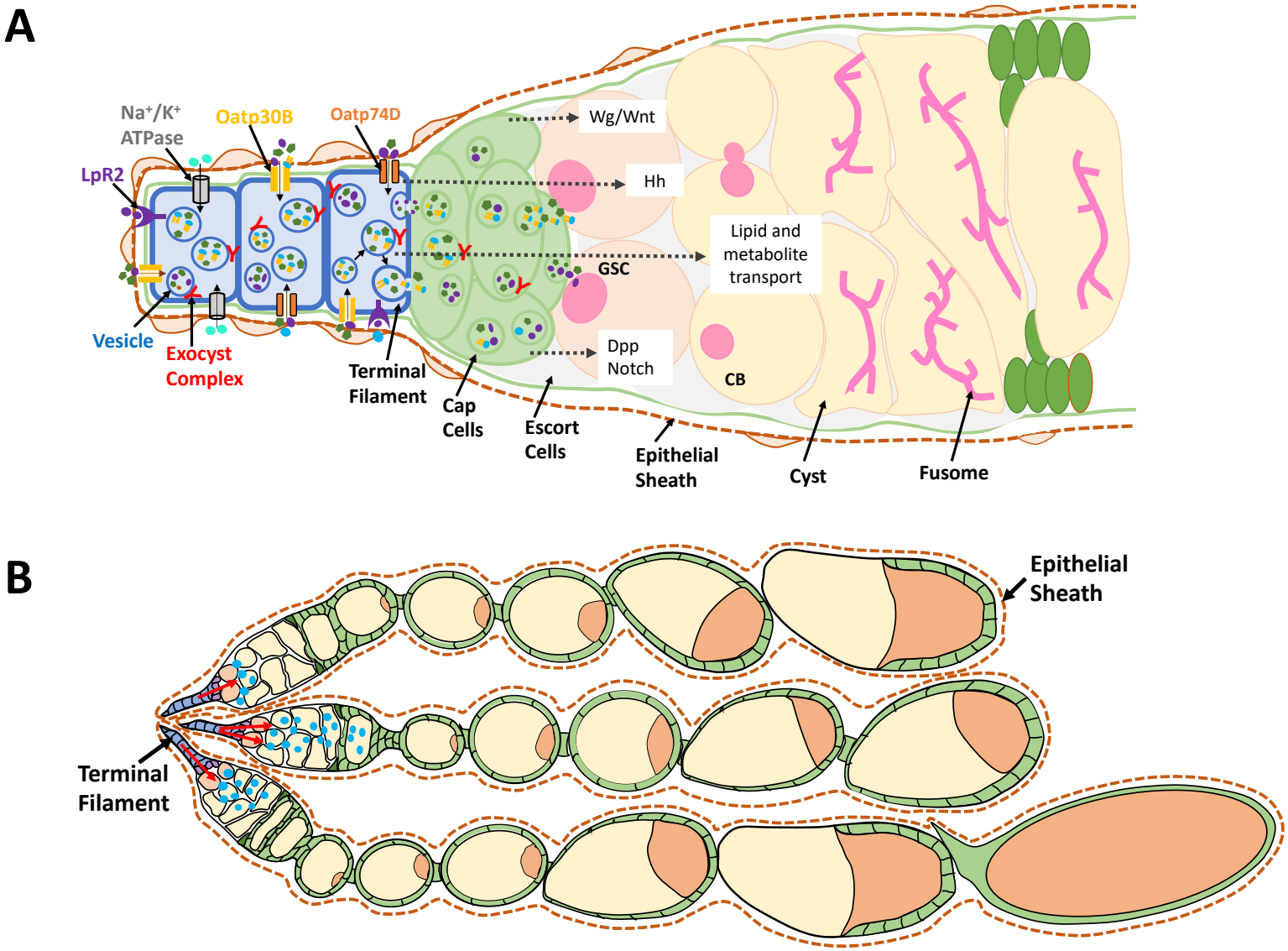
A
Na+/K+ ATPase
Oatp30B
Oatp74D
LpR2
Wg/Wnt
Hh
Lipid and metabolite transport
GSC
Dpp
Notch
CB
Vesicle
Exocyst Complex
Terminal Filament
Cap Cells
Escort Cells
Epithelial Sheath
Cyst
Fusome
B
Epithelial Sheath
Terminal Filament

Fig.7